Wright Brothers Lectureship in Aeronautics AIAA 80-1836R

Turbulent Wind and Its Effect on Flight

B. Etkin
University of Toronto, Toronto, Canada

Nomenclature

g	= gust vector
L	= lift, rolling moment, integral scale of isotropic turbulence
(p, q, r)	= components of ω in F_B
$(p_g, q_g, r_{1_g}, r_{2_g})$	= $(\partial w_g/\partial y, -\partial w_g/\partial x, -\partial u_g/\partial y, \partial v_g/\partial x)$
u	= control vector
(u, v, w)	= components of V in F_B
(u_g, v_g, w_g) or (u_1, u_2, u_3)	= components of $(W - W_A)$ in F_B or F_A
(u_g', v_g', w_g')	= components of W in F_E
V	= velocity of airplane mass centre relative to F_A
V_e	= reference steady value of V
W	= local velocity of the air relative to the Earth
W_A	= mean value of W, velocity of frame F_A
x	= state vector
X_u, etc.	= $\partial X/\partial u$, etc., classical stability derivatives
λ_i	= wavelength, $2\pi/\Omega_i$
σ	= rms value of stochastic variable indicated by subscript
ξ	= vector separating two points in F_A
ω	= angular velocity of airplane relative to F_E
ω_A	= local angular velocity of air relative to F_E
Ω $(\Omega_1, \Omega_2, \Omega_3)$	= wave number vector in F_A
$\theta(\Omega_1, \Omega_2, \Omega_3)$	= matrix of three-dimensional spectrum functions
$\Psi(\Omega_1, \Omega_2)$	= matrix of two-dimensional spectrum functions
$\Phi(\Omega_1)$	= matrix of one-dimensional spectrum functions
$\bar{(\ )}$	= Laplace transform
$(\ )^T$	= transpose of matrix
$\langle\ \rangle$	= ensemble average
$(\ )^*$	= complex conjugate

Reference Frames

F_E: (x_E, y_E, z_E)	= Earth-fixed frame: ox_E *points in direction of mean wind,* oz_E vertical down
F_A: (x_1, x_2, x_3)	= frame convected with the mean wind at velocity W_A
F_B: (x,y,z)	= vehicle-fixed frame

Introduction

IN the earliest days of aeronautical experimentation, the natural wind proved itself to be a major obstacle to successful flight. Certainly one of the prime hurdles that had to be overcome by Wilbur and Orville Wright was maintaining a wings-level attitude in the presence of side gusts. These two incomparable applied scientists and inventors, when faced with this problem, recognized the distinction between gust response and stability in still air, and the need for a tradeoff between them. To quote Orville Wright, testifying in a patent lawsuit in January 1920,[1] commenting on their use of negative wing dihedral to improve the gust response: "This, however, tends to produce a machine with unstable equilibrium laterally. While the equilibrium is disturbed less from side gusts, the machine tends to lose its own equilibrium when it slips sideways in the air." In this, as in so many other aspects of their remarkable accomplishment, the brothers displayed the sure grasp of fundamentals that was the hallmark of their work. The subject of this paper therefore seems very appropriate for a lecture commemorating the Wright Brothers, and I consider myself most honored to be this year's lecturer.

The achievement of successful flight by the Wrights did not end the problem of gusty winds. The early history of aviation abounds with incidents and accidents in which the variability of the wind in space or time played a decisive role. Loss of control of the attitude or of the flight path, and failures of structure were not uncommon. There are still too many turbulence- and shear-related accidents; we still do not know

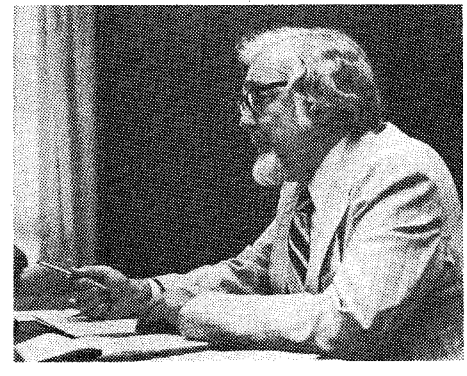

Professor Bernard Etkin was born and educated in Toronto, Canada. He has served the University of Toronto as a Professor of Aerospace Engineering, Department Chairman, Faculty Dean, and member of its Governing Council. His professional experience has included participation in the design and/or manufacture of some 12 airplanes and gliders. He has done research in structures, aerosonics, aerodynamics, particle dynamics, satellite dynamics and atmospheric flight mechanics. He has served on a number of government bodies and is Chairman of Transport Canada's Aeronautics Advisory Board. He is currently a Professor in the Institute for Aerospace Studies.

Presented as Paper 80-1836 at the AIAA Aircraft Systems Meeting, Anaheim, Calif., Aug. 4-6, 1980; submitted Sept. 10, 1980. A much expanded version of this paper has been published as University ofToronto UTIAS Review 44. It contains much material not included here because of limitation of space.

enough about the atmosphere—even something as basic as the "correct" value of the integral scale of atmospheric turbulence eludes us; methods of aerodynamic and structural analysis and design continue to be refined and improved; guidance and control systems are evolving rapidly; and vehicle configurations undergo constant evolution and innovation, from wide-bodied jets to VTOL and hybrid lighter-than-air vehicles. All of these factors make it necessary for us continually to re-examine and improve our analytical and experimental modeling of the atmosphere for application to design and flight simulation. Moreover, the recent explosive growth in computing capability has exerted a powerful influence on all aerospace activities and has provided unprecedented opportunities for sophisticated analysis, control, and simulation. An intense interest in the turbulent wind, which has been part of the aviation scene from the time of the Wrights to the present day, will no doubt be with us as long as there are vehicles flying in the air.

This subject was recognized as a very high priority item by NACA when it was originally established. Part 2 of its very first report in 1915 was entitled "Theory of an Aeroplane Encountering Gusts,"[2] prepared by E.B. Wilson of M.I.T. Wilson's paper contains much of the basic analysis that is current today: the relevant equations of motion in body axes, the linearization to small disturbances, the expansion of aerodynamic forces in terms of stability derivatives, the encounter with discrete gusts of varying rise time, and the multidimensional nature of the wind. The last item was expressed through the introduction of six linear and rotational air motions in the following terms: "We should in general allow a gust to have components u, v, w, p, q, r relative to the axes. This would take into account any possible rotational motion in the gust." He goes on to say, "It may well be that the rotational element is of great importance." He arrived at this conclusion by noting the very large values of the derivatives L_p and M_q. In this analysis he anticipated by nearly 50 yr those of us who took account of streamwise and spanwise variation in gust velocity by treating them as equivalent rates of pitch, roll, and yaw. The mathematical and computing methods used by Wilson were of course primitive, being those current in the second decade of this century. His calculations were done by hand using four-place log tables, the computational burden being therefore so heavy that he presented a total of only 10 graphs of results. These cover examples of responses to u, w, and q gusts.

My own interest in the mechanics and aerodynamics of flight in a wind goes back to the 1940s.[3,4] (This was not unrelated to the fact that I was the pilot of a training glider that crashed in a tail-wind landing in 1942.) Wind gradients and turbulence have been topics of recurring activity over the years since.[5-10] There have of course been many contributions to the theoretical and practical development of this subject. I make no attempt to present an accurate historical analysis of this development nor to weigh the relative merits of the many contributions, but simply comment that I was myself much influenced by certain landmark reports by Press, Houbolt, and others[12-14,21] at NASA Langley and by basic theoretical papers by Liepmann[15,16] and Ribner.[17]

What then are the problems that so concerned our predecessors and continue to absorb aeronautical engineers today? The main ones are:

1) Strength: The part played by gusts and turbulence in loading vehicle structures.

2) Controllability: The ability of the human or automatic pilot to maintain the required trajectory and attitude of the vehicle, especially to be able to land safely in a strong turbulent wind or strong wind shear.

3) Structural fatigue: The accumulation of fatigue damage resulting from very large numbers of cycles of stress associated with rigid body and structural mode responses to turbulence. Fatigue cracks, as some accidents have shown, can be insidious and escape detection.

4) Handling qualities: The effect of turbulence on the pilot, in producing human fatigue and lowering his effectiveness and his rating of the airplane.

5) Passenger and crew safety and comfort: Ride roughness is of course undesirable from the simple standpoint of a pleasant ride. When severe enough, however, it can in fact be dangerous and result in injury to cabin crew and passengers.

Apropos of item 5, there has been a surprisingly large number of accidents in which turbulence has been cited as a factor. Brunstein[22] reports that of 729 accidents reported by U.S. air carriers in the years 1964-1975, 183 (25%) were turbulence related. Of these, 115 occurred in convective turbulence (including storms) and 68 in clear-air turbulence (CAT). "Accident" in this context means "...a person suffered death or serious injury or the aircraft suffered substantial damage or was destroyed." The cabin crew were identified as those at relatively greatest risk, and the galley and lavatory areas as the most dangerous since persons in those areas are least likely to be restrained. Most of the CAT occurrences were in cruising flight at about 30,000 ft. The cost to the airlines of CAT accidents was estimated in 1972 to be of the order of $23 million annually.

The "structure" of the gust-response problem is conveniently subdivided into several parts, as illustrated in Fig. 1. The first block refers to the description of those motions of the air that are of interest. These relate to a variety of meteorological conditions: clear air turbulence, convective/storm turbulence (e.g., thermals and downbursts), mountain waves, boundary-layer turbulence, and shear over various terrains. The second block relates to the purely aerodynamic problem of converting a prescribed velocity field in space and time into the forces and moments that drive the rigid-body and structural degrees of freedom. Finally, the remaining blocks relate to the computation and assessment of the responses to the forces. Pervading all these steps in the practical business of building airplanes is the ever-present influence of the certifying authority, civil or military, which normally prescribes crucial parameters of the gust/turbulence model employed and the levels of response that are acceptable.

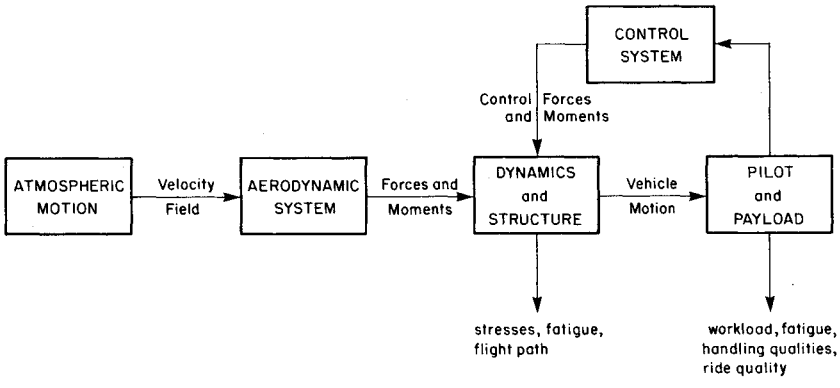

Fig. 1 Structure of the gust-response problem.

Finally, it should be noted that designers do not have to accept undesirable responses as immutable. Design changes can ameliorate the gust response of airplanes, as the Wrights demonstrated. In fact, with modern automatic control technology, very substantial gust alleviation is readily achieved for the rigid-body degrees of freedom, and advances have been demonstrated in reducing structural responses as well, as for example in the B-52 and C-5A programs.[23] Large reductions in fatigue damage rate can be obtained with an active load alleviation system.

Description of the Turbulent Wind

The medium of flight is the relatively thin layer of air that envelopes the Earth (practically speaking, only about 1% of its diameter). This atmosphere is driven into intricate motion by Earth rotation and solar heating, and is host to a variety of complex thermodynamic, chemical, and electromagnetic processes. The turbulence associated with the motion is of prime concern to engineers not only because of its effect on aircraft, but also in relation to ground-based structures and the dispersal of pollutants. A review of its nature and causes was given in 1972 by Houbolt.[24]

So complex and so many-faceted are the phenomena that take place in the atmosphere that any nonmeteorologist may be forgiven for approaching a description of it with some trepidation. As I contemplated this difficulty, I was inspired to set down a few lines of verse, which, with apologies to Elizabeth Barrett Browning, I now share with you:

The Turbulent Wind

How do I describe thee? Let me count the ways.
By compass, speed, and frequency,
By space embraced, and length of stay,
By gust and probability.
For shear and downburst, cloud and storm,
Discrete or random, which is norm?
Let those who feel that they must choose
Between the single and diffuse,
Reflect.
No single rule should we expect
To guide us through the whole design.
For weather's but an Earthly sign,
Reflection.
Of God's infinite complexion.
Within the universe of choice
Both cos and Φ must have a voice
In helping humankind to fly
With gentle safety in the sky.

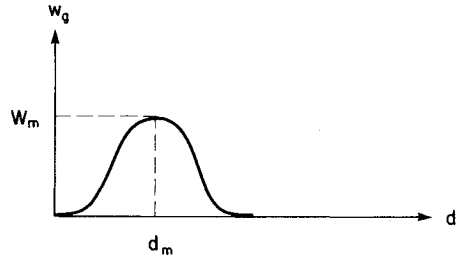

Fig. 2a The (1 − cos) gust shape.

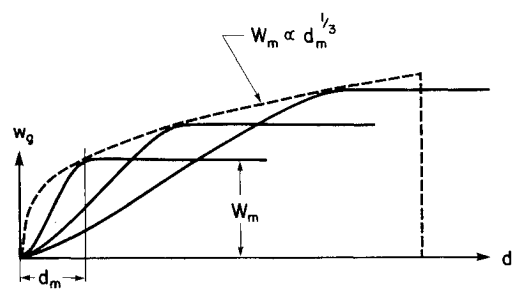

Fig. 2b Family of equiprobably gusts (after Jones, Ref. 28).

It is of course very important to keep our goals clearly in mind as we approach the task of describing the wind. The *scientific* goal is to get at the truth of what it is, and an understanding of why it is so. The goal of aeronautical engineers is to design and operate airplanes safely. To this end we need engineering models of the wind that are satisfactory for design and analysis, we need to know what conditions are dangerous for flight, and we need warning systems to enable us to avoid these dangerous conditions. It is a great help that for many applications the engineering models need to describe only the "worst case"—the largest gust, the most intense turbulence, the worst shear that is encountered with some specified low probability. When structural fatigue is the issue, the "worst-case" philosophy is not so simply applied. The rate of accumulation of fatigue damage depends of course on the particular missions or routes on which an airplane is used. But these are not in general predictable in advance of production. To design for the worst possible operational life history many unduly penalize a whole fleet, since where fatigue is concerned, inspection intervals can be adjusted to allow for different operating conditions.

Physical reality matters because the models we use will be truly successful only if they are intelligently related to it. Otherwise, new departures in design will be risky. Nevertheless, engineering models do not have to reflect *all* of the true variability of the wind. Safe and economical designs of airplanes have been made with the fairly simple models evolved over the seven decades since the Wrights first flew. Progress in this area will result from continually improving the models themselves and improving the techniques for applying them to design. Insofar as application is concerned, undoubtedly the most significant development since Wilson's report has been the advent of truly massive computing power which makes it possible to use sophisticated wind models in conjunction with elaborate airplane models.

Our models of the wind have to accommodate both events that are perceived as discrete (usually described as gusts), as well as the phenomenon described as continuous turbulence. These two are discussed separately below, even though some "discrete" gusts are actually the rare extreme excursions that occur in continuous turbulence.

Discrete Gusts

Discrete events are isolated encounters with steep gradients (horizontal or vertical) in the horizontal or vertical speed of the air. These gradients may occur at the edges of thermals and downdrafts; in the wakes of structures, mountains, hills, or cliffs; or at temperature inversions. They may also appear as rare extremes of turbulence in clouds, storms, and the jet stream, possibly associated with organized structures embedded in the otherwise chaotic background. These turbulence extremes are not adequately allowed for in the usual

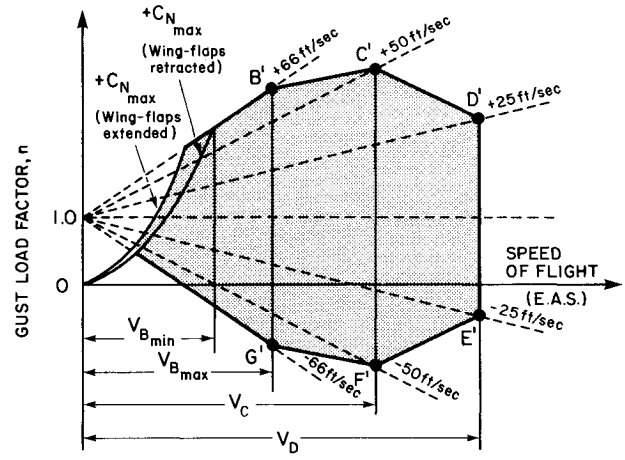

Fig. 3 Gust envelope for altitude ≤20,000 ft.

Gaussian models of continuous random turbulence. Finally, the tip vortices of other aircraft are a man-made source of shear. When an airplane penetrates any of these gradients rapidly enough to produce a strong change in the aerodynamic field experienced by the vehicle, the consequence will be changes in load, attitude, and trajectory that have to be understood and taken into account.

The discrete gust has evolved over the years from the isolated sharp-edged step-function used in the earliest airworthiness requirements to the currently favored $(1-\cos)$ form (Fig. 2), in which w_g is the gust velocity and d is distance along the flight path. The severity of the gust is controlled by the magnitude of W_m and d_m. Typical of the philosophy for choosing these parameters is the specification for vertical gusts of the U.S. Federal Air Regulations, which may govern the design of much of the structure. This fixes $2d_m$ as $25\bar{c}$ and gives a number of values of W_m corresponding to a set of defined speeds on the "gust envelope" (Fig. 3). The British regulations (ARB CAR Ch. D3-3) use the identical gust envelope, but specify that the distance d_m "...shall be varied to find the peak responses along the wing span." This significant addition is made to account for the dynamic amplification of stress that can result when a transient load is applied to a flexible structure. Unsymmetrical vertical and side gusts that generate rolling and yawing moments are also commonly specified in airworthiness requirements. The requirements display large differences between the strength of gusts specified at different flight speeds. This could be taken to imply that airplanes fly at lower speed when there is a significant probability of encountering a large vertical gust. If the environment immediately preceding the extreme event is such as to give warning of it, then a reduction of speed is a logical presumption. If, on the other hand, the discrete gust is truly an isolated event encountered without warning, then clearly its strength cannot be a function of the speed of the airplane. This is a situation that actually does occur. The validity of this form of specification really rests on accumulated experience—airplanes with structures designed to the specified load factors have been found to be strong enough in the past, and may therefore be expected to be satisfactory in the future as well.

The use of discrete gusts for structural design has been carried to a high level of sophistication by Jones et al.[25-28] at the RAE. Jones has noted the crucial role of gradients in the air velocity (a uniform and constant wind produces only navigational disturbances, without affecting loads or attitude). He found that the differences in vertical gust speed between points horizontally separated by distances of interest for airplanes have probability distributions that are strongly non-Gaussian. For example, in thunderstorm turbulence a $4\frac{1}{2}\sigma$ vertical gust difference that occurs with a Gaussian probability of 7×10^{-6} may in reality have a probability many times larger.[28] This is in a situation wherein the gust velocity itself appears to have a nearly normal distribution up to $\pm3\sigma$. This should *not* be taken to mean that probabilities based on Gaussian distributions specified by authorities [see Eq. (12)] are not credible. For such probabilities are specified in the context of a total certification model that contains other parameters chosen in such a way that the result is compatible with prior art and existing satisfactory airplanes. In the basic model proposed by Jones, the gust is like the first half of the $(1-\cos)$ form; its magnitude W_m varies as $d_m^{1/3}$, and the frequency of encounter is given by

$$N(W_m, d_m) = \frac{\alpha}{d_m^2}\exp\left(-\frac{W_m}{1.15\beta d_m^{1/3}}\right)$$

That is, $N(W_m,d_m)\,\delta d_m$ is the number of discrete gusts per unit distance flown for which d_m lies in range δd_m and whose maximum is greater than W_m. α and β are parameters that fix the family of gusts to be described—α a frequency parameter and β an amplitude parameter. The exponential form of N is a realistic non-Gaussian probability distribution for the velocity differences. This is the basis of the "statistical discrete gust" (SDG) model of turbulence. At any given probability level, one can choose the "worst" gust from an (almost) equiprobable family having different W_m and d_m (Fig. 2b). A single such ramp gust is adequate to find the response of a heavily damped airplane mode (i.e., one with cycles to ½ amplitude less than about 0.2). The maximum response then corresponds to a "tuned" gust of the right d_m, a point that has been incorporated, as noted above, in British airworthiness requirements. For lightly damped modes, a succession of gusts suitably spaced is required to generate the appropriate resonant buildup.

Random Turbulence

Random turbulence is a chaotic motion of the air (Fig. 4) that is described by its statistical properties. The main statistical features that need to be considered are: stationarity, homogeneity, isotropy, time and distance scales, probability distributions, and correlations and spectra. Moreover, unlike simpler scalar random processes in which there is only one dependent and one independent variable, to which the above list of statistical features also apply, turbulence is a vector process in which the velocity vector is a random function of the position vector and of time. Because of the complexity introduced by this multidimensionality, the description of turbulence and the associated input/response problems are often simplified (whether justified or not!) to a one-dimensional representation. Much has been written on the statistical properties of turbulence,[6,21,24] and only the

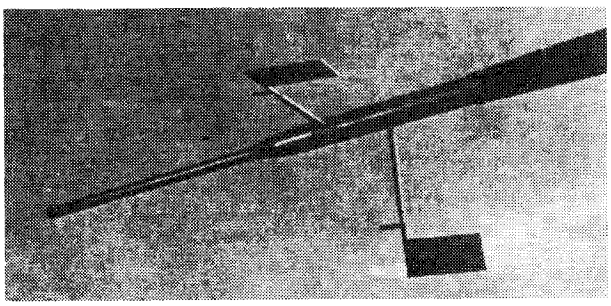

Fig. 4a NASA probe used in flight measurements of turbulence.

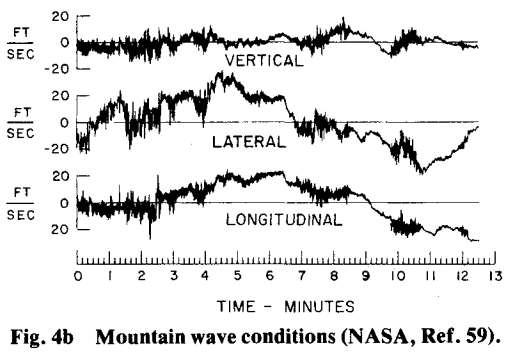

Fig. 4b Mountain wave conditions (NASA, Ref. 59).

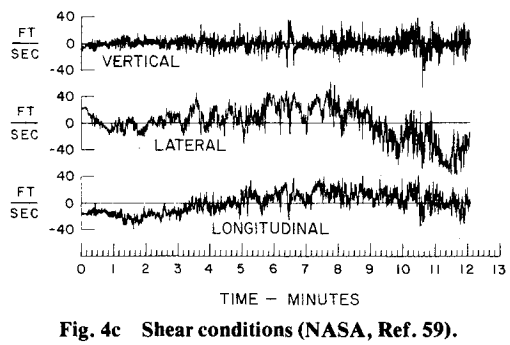

Fig. 4c Shear conditions (NASA, Ref. 59).

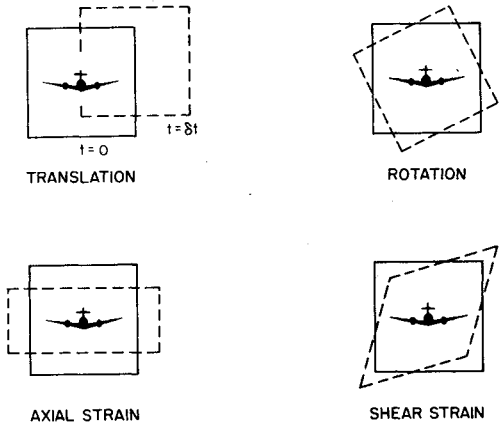

Fig. 5 Movement of the air mass around vehicle in two dimensions.

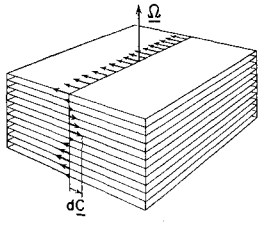

Fig. 6 Sinusoidal wave of shearing motion (Ribner, Ref. 24).

minimum necessary for completeness is repeated here. (Much more detail is given in UTIAS Review 44.)

It is difficult to visualize the physical implications of the random vector field, and yet we know from observing smoke, leaves, and snow swirling in the wind, that there is some spatial organization to turbulent motion. Recognizing that the scale of atmospheric turbulence is usually fairly large in comparison to flight vehicles, we can get some help from a classical theorem.[30] This says that in a "small" region we can regard the velocity as a linear function of distance. It then follows that in this region the motion is a superposition of three simple basic fields: translation, rotation, and strain, i.e.,

$$W(r) = W_0 + \tilde{\omega}_A r + E_1 r + E_2 r \tag{1}$$

Here W is the wind velocity vector at r, W_0 is its value at the origin, and $\tilde{\omega}_A$, E_1, E_2 are matrices containing the nine velocity gradients as elements. $\tilde{\omega}_A$ represents solid-body rotation of the air, and E_1 and E_2 are axial and shear rates of strain. Figure 5 illustrates the motion of the air in two dimensions that is represented by Eq. (1). Instead of chaos, we find beautiful order in the microscale! Wilson's[2] use of p, q, and r was a way of recognizing the $\tilde{\omega}_A$ part of this general motion.

The term "point approximation" has been used in the past to describe the case when the turbulent velocity can be assumed to be constant over the airplane, i.e., when W_0 is the only term that needs to be retained in Eq. (1). It is true that the assumption of uniform velocity can be made with little loss in accuracy when the scale of atmospheric turbulence is large (as at high altitude). This is because the components of E_1, E_2, and $\tilde{\omega}_A$ become small as the scale becomes large. On the other hand, in a turbulent field in which these components are not negligible, allowing the airplane to become vanishingly small does *not* reduce the importance of the shear and rotation. In that case the point approximation is truly represented by Eq. (1), which therefore may be expected to apply to the flight of model airplanes, birds, and insects in small-scale turbulence close to the ground where E_2 and $\tilde{\omega}_A$ are important.

A quite different view of the "organization" of turbulence is provided by the spectral decomposition of the three-dimensional vector field.[17] Figures 6 and 7 illustrate the

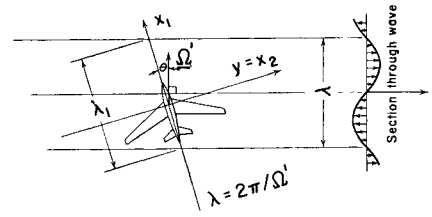

Fig. 7 Elementary spectral components in two dimensions (Ribner, Ref. 24).

concept. A single spectral component of the turbulent field (Fig. 6) is a "wave" of shearing motion with wave number Ω and complex vector amplitude dC perpendicular to Ω. The velocity in this wave at position r is given by

$$dW = e^{i(\Omega^T r)} dC \tag{2}$$

One component, such as vertical gust w_g is then

$$dw_g(r) = e^{i(\Omega^T r)} dc_3$$

where dc_3 is the component of dC on ox_3. Figure 7 shows how this component relates to a (planar) airplane flying through it. The nodal planes of the wave intersect the plane of flight (the x_1x_2 plane) in the nodal lines shown, with wavelength $\lambda = 2\pi/\Omega'$. Ω' is the projection of Ω on the x_1x_2 plane. If the vehicle penetrates the field at speed V, so that with (x,y) coordinates attached to the vehicle $x_1 = x + Vt$, and $x_2 = y$, we get

$$dw_g(t,x,y) = e^{i\Omega_1 Vt} e^{i(\Omega_1 x + \Omega_2 y)} dc_3 \tag{3}$$

Similar expressions give the other velocity components du_g and dv_g. The gust velocity is thus seen to be periodic in time at any point on the airplane with frequency $(\Omega_1 V/2\pi)$ and "wavy" over the airplane at any time. The total turbulent field is made up of a superposition of spectral components such as those of Fig. 6, just as a Fourier series represents a random scalar in one dimension.

Model of Turbulence at Altitude

The engineering model of random turbulence at altitude has been developed over many years and is well described in the existing literature.[6,21,24] It is now widely accepted that it is satisfactory to treat it as frozen, homogeneous, and isotropic in relatively large patches. The frozen-field assumption, closely allied to Taylor's hypothesis, is that turbulent velocities do not change during the time of passage of the airplane. This is a valid assumption for all but near-drifting speeds, i.e., $V/W \geq 1/3$. It is usually assumed that either the Dryden[21,31] model or the von Kármán model[21] describes the correlation and spectra adequately, with the weight of experimental evidence favoring the latter. Finally, although there is much evidence that turbulence is not in fact a Gaussian process, with small and large values both occurring more frequently than in a normal distribution, the assumption that individual patches are Gaussian is widely used because of the great analytical advantage it offers.

The principal relations and equations pertaining to isotropic turbulence needed are listed below for reference:

Correlation matrix:

$$R_{ij} = \langle u_i(r,t) u_j(r+\xi, \tau+\tau) \rangle$$

$$= \sigma^2 \left\{ [f(\xi) - g(\xi)] \frac{\xi_i \xi_j}{\xi^2} + \delta_{ij} g(\xi) \right\} \tag{4}$$

where $f(\xi)$ and $g(\xi)$ are the longitudinal and transverse correlation functions, respectively, $\xi^2 = \xi_1^2 + \xi_2^2 + \xi_3^2$, and

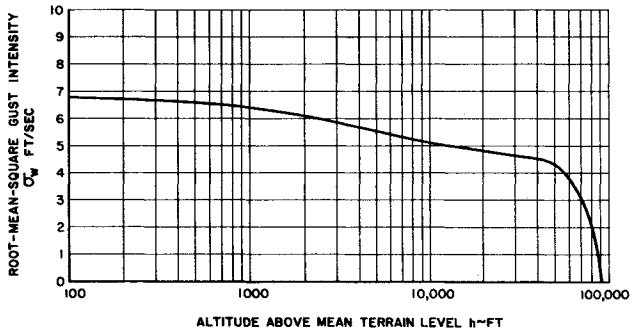

Fig. 8 Intensity of clear air turbulence (USAF MIL Spec. 8785).

$\sigma^2 = \overline{u_g^2} = \overline{v_g^2} = \overline{w_g^2}$, the (intensity)^2 of the turbulence. f and g for the von Kármán model are given in Ref. 6 and UTIAS Review 44.

Spectrum matrix*

$$\theta_{ij}(\Omega) = \frac{E(\Omega)}{4\pi\Omega^4}(\Omega^2\delta_{ij} - \Omega_i\Omega_j) \tag{5}$$

$$E(\Omega) = \frac{55}{9\pi}\sigma^2 L \frac{(aL\Omega)^4}{[1+(aL\Omega)^2]^{17/6}} \tag{6}$$

θ_{ij} is the three-dimensional spectrum function and E the energy spectrum of which Eq. (6) is the von Kármán form. θ_{ij} and R_{ij} are a Fourier transform pair. Two- and one-dimensional spectra are obtained from θ by successive integration with respect to Ω_3 and Ω_2. The familiar one-dimensional spectra often given in the literature for the von Kármán model of turbulence are

Longitudinal

$$\Phi_{11}(\Omega_1) = \frac{\sigma^2 L}{\pi} \frac{1}{[1+(aL\Omega_1)^2]^{5/6}} \tag{7}$$

Transverse

$$\Phi_{22}(\Omega_1) = \Phi_{33}(\Omega_1) = \frac{\sigma^2 L}{2\pi} \frac{1+(8/3)(aL\Omega_1)^2}{[1+(aL\Omega_1)^2]^{11/6}} \tag{8}$$

All other Φ_{ij} are zero because of isotropy, and as $\Omega \to \infty$ these spectra $\sim\Omega^{-5/3}$ as required by the Kolmogoroff theory of turbulence.[32] Even in isotropic turbulence, however, the Ψ_{ij} are not all zero for $i \neq j$.

In the above expressions, L is the integral scale of the turbulence. It is the area under the $f(\xi)$ curve. The area under $g(\xi)$ is the transverse scale, and is exactly $L/2$. With the prior stipulations, the model is completed by specifying the two parameters L and σ.

The determination of L at altitude remains an unresolved difficulty. Early estimates suggested a value of about 300 m. Some subsequent studies indicated larger values, and others smaller ones. Values as large as 1500 m and as small as 150 m have been proposed.[24] The problems that plague this determination have to do with method of approach—whether to find L from the area under a correlation curve or from a fit to a spectrum—and with the bandwidth of the data. There are large variations in the wind that occur slowly, and how to handle this low-frequency component of the data presents a problem. Fortunately, the portion of the spectrum that matters most for airplane design is limited, the very low frequencies that cause the problem for L not being very important. As noted in the following, the values currently being specified by regulatory authorities are rather large. Since the effect of L is important for airplane response, and in keeping with the "worst-case" philosophy it may well be that a *range* of L should be specified for proof of structure and handling qualities, rather like the ARB requirement for "tuned" gusts.

*Note that the spectra used here are two-sided spectra, for which

$$\sigma^2 = \int_{-\infty}^{\infty} \Phi(\Omega_1)\,d\Omega_1 = 2\int_0^{\infty} \Phi(\Omega_1)\,d\Omega_1$$

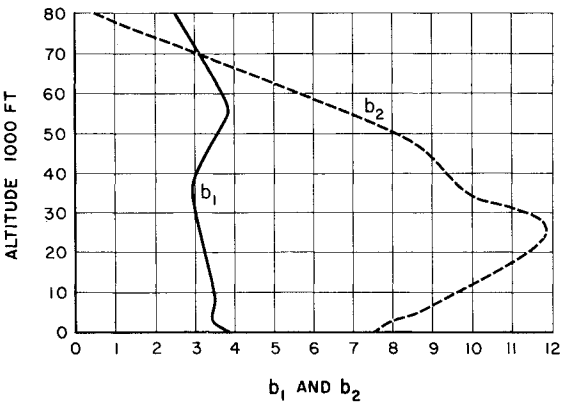

Fig. 9 Values of b_1 and b_2.

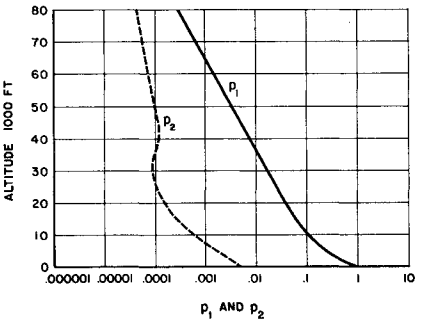

Fig. 10 Values of p_1 and p_2.

High-altitude measurements show that the probability of encountering turbulence with σ of $\sim$ 3 m/s in CAT or $\sim$ 8 m/s in storms is about 10^{-6}. The U.S. Air Force[31] specifies a σ in CAT that varies with altitude to be used in studies of flying qualities (Fig. 8). The maximum value is about 7 ft/s (2.1 m/s) based on an exceedence probability of 0.01. It also specifies σ = 21 ft/s (6.4 m/s) for storm turbulence. The same specification requires the integral scale L to be 2500 ft (762 m) in the von Kármán model and 1750 ft (533 m) in the Dryden model. These scales are used for both CAT and thunderstorms. The numerical difference between the two scales results from the different matching of the two forms of spectrum to experimental data.

The FAA requires, in relation to structures of transport airplanes (FAR-25, 25.305), that "The dynamic response of the airplane to vertical and lateral continuous turbulence must be taken into account." A current industry proposal for compliance utilizes by implication the previously described von Kármán model with $L = 2500$ ft (762 m) and either of two methods of analysis as follows:

1) *Design envelope analysis.* This is based on a particular gust velocity† U_σ and on the dynamic response parameter

$$\bar{A} = \sigma_x/\sigma_w \tag{9}$$

σ_x is the rms value of the response to continuous random turbulence of the variable in question (e.g., wing bending

†This inappropriate notation is now unfortunately entrenched in the documentation and in practice.

moment), and σ_w is the rms value of the vertical component of turbulence. The design load is then specified to be

$$x_{\text{des}} = \bar{A} U_\sigma \tag{10}$$

What this implies is that U_σ is $m\sigma_w$ and hence that

$$x_{\text{des}} = (\sigma_x/\sigma_w)\, m\sigma_w = m\sigma_x \tag{11}$$

The value of m is not specified. Instead, the model (which now combines *both* the turbulence intensity *and* the probability of experiencing an extreme value) is completed by specifying pairs of U_σ and flight speed V for various altitudes, configurations, and weights. The U_σ values corresponding to the discrete gusts shown on Fig. 3 are exactly 1.5 times the gust values shown there. As with the discrete gust specifications, there is an implication that speed is reduced when intense turbulence is encountered.

2) *Mission analysis.* This is based on the probability distribution of encountering turbulence in representative flight operations. $p_1(h)$ and $p_2(h)$ are defined as the probabilities of encountering nonstorm and storm turbulence, respectively, at altitude h, and $b_1(h)$ and $b_2(h)$ are corresponding intensity parameters (see Figs. 9 and 10). The design load is then that load which is exceeded at a frequency of 2×10^{-5}/h. The formula for calculating exceedences is obtained by assuming that the total flight is a sum of Gaussian patches.[21] The result is

$$N(x) = \Sigma t N_0 \left[p_1 \exp\left(-\frac{|x - x_{\text{ref}}|}{b_1 \bar{A}} \right) + p_2 \exp\left(-\frac{|x - x_{\text{ref}}|}{b_2 \bar{A}} \right) \right] \tag{12}$$

where:

x	= net value of load or stress
x_{ref}	= value of x in 1 g level flight
$N(x)$	= average number of exceedences of the indicated value of x in unit time
N_0	= number of zero-crossings of x per unit time (equal to the radius of gyration of $\Phi_{xx}(\omega)$ about zero frequency)
$\bar{A}$	$= \sigma_x/\sigma_w$
t	= fraction of time in mission segment
Σ	= summation over all mission segments

The dynamics of the vehicle enters the analysis through the computation of the response parameters $\bar{A}$ and N_0.

Unlike the design envelope approach, the mission analysis approach provides data that can be used for fatigue strength calculations as well as for limit load design.

Model of the Atmospheric Boundary Layer

The wind conditions that exist close to the ground, within the Earth's boundary layer (a thickness not precisely defined, but for engineering purposes roughly up to 600 m), are characteristically very different from those at higher altitude and are governed by quite different parameters. An excellent account of this subject is given in Ref. 33. Coupled with these differences between low and high altitude is the fact that aircraft are normally taking off or landing when in this regime, and hence the engineering problem is also quite different—speeds are at the low end of the range, flaps and landing gear are extended, flight path control is crucial, and the consequences of something going wrong are likely to be catastrophic.

In recent years, the boundary layer has received much attention, especially from groups interested in wind loads on ground-based structures[33] and in the dispersion of pollutants. Excellent reviews that summarize the known data are given in Refs. 33-37.

The principal factors that govern the wind structure (profiles of mean wind, turbulence intensities, and turbulence scales) are the roughness and uniformity of the underlying terrain and the thermal stability of the atmosphere. Airports frequently present a sudden rough-to-smooth transition upwind of runways so it is not easy to obtain generally applicable data. Thermal stability is a powerful factor in fixing turbulence characteristics at low wind speeds, but for high winds, the case of most interest to us, a "neutrally stable" atmosphere is a good approximation. The following description therefore pertains only to neutral stability and uniform roughness over a long upwind fetch. The velocity components (u_g, v_g, and w_g) are downwind, crosswind, and vertically down.

The Mean Wind

The mean wind profile very close to the ground is found to be governed mainly by surface roughness, and is well approximated by the logarithmic law (the law of the wall):

$$\frac{W}{u_*} = \frac{1}{k} \ell n \frac{h-d}{z_0} \tag{13}$$

where:

W	= mean wind speed at height h
u_*	= friction velocity
k	= von Kármán's constant = 0.4
z_0	= surface roughness length
d	= displacement of the zero plane

The friction velocity u_* is related to the surface friction stress by

$$\tau_0 = \rho u_*^2 \tag{14}$$

Values of u_*, d, and z_0 are obtained experimentally by fitting measured profiles of W vs h to Eq. (13). When a suitable value of d has been determined a plot of W vs $\ell n\,(h-d)$ will be a straight line, from the slope and intercept of which z_0 and u_* can be inferred. Values of z_0 vary from as low as about 10^{-4} m for calm open water to as large as 3 m for urban areas. The logarithmic law is used mainly for these experimental determinations. Measured boundary-layer profiles display great variability resulting from differences in terrain features and meteorological conditions. A simple form of power law has therefore been found to provide a satisfactory engineering model, i.e.,

$$W/W_{\text{ref}} = (h/h_{\text{ref}})^\alpha \tag{15}$$

The power law index α is a function of roughness height, varying from about 0.10 for a smooth surface to about 0.40 for urban centers, see Fig. 11.[37] Although the mean wind direction usually veers with height, the basic model assumes that the wind vector does not change direction in the boundary layer. Sharp changes of direction with height (heading shear) are nevertheless possible, and need to be considered as part of the wind shear problem.

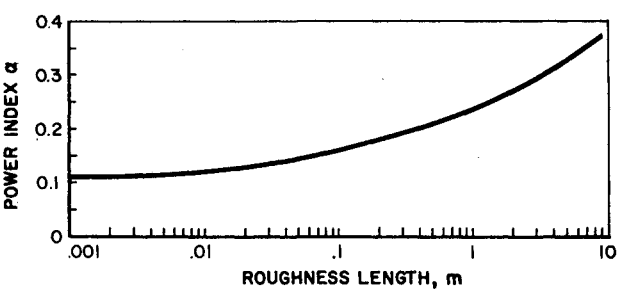

Fig. 11 Variation of the power law index with roughness.

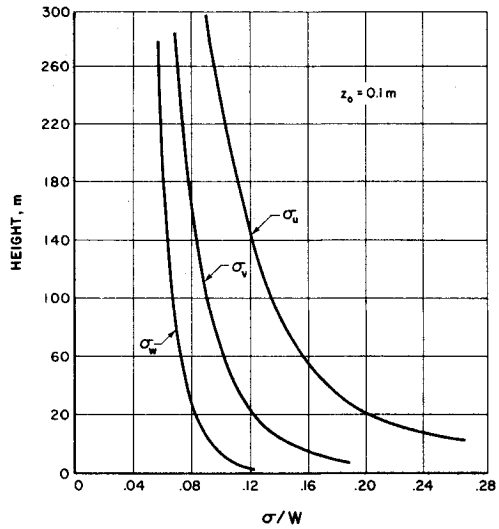

Fig. 12 Turbulence intensities for ESDU model, $z_0 = 0.1$ m.

Turbulence Intensities

In the "surface layer," i.e. the layer close to the ground (about 10% of the boundary layer) in which the shear stress is assumed to be constant, the three turbulence intensities are unequal, their ratios being a function of surface roughness and altitude and ordered as,

$$\sigma_u > \sigma_v > \sigma_w$$

Above the surface layer, the three intensities decrease and tend to equality outside the boundary layer (at about 300-1000 m). Finally, the presence of the surface shear stress means that the correlation $R_{uw} = \overline{u_g' w_g'}/\sigma_u \sigma_w$ does not vanish, since $\overline{u_g' w_g'} = u_*^2$.‡ The data suggest that $R_{uw} \approx 0.3$ as a typical value. Figure 12 shows typical intensities derived from Ref. 35, plotted as ratios of turbulence to average wind speed at the given height.

Scales

In the anisotropic boundary layer, we have to consider more than the two integral scales that characterize isotropic turbulence. There is a scale associated with each correlation of the i component of velocity as measured by two probes separated on the j axis. This is denoted L_i^j, where we use $[u, v, w]$ for i and $[x, y, z]$ for j. There is some information available about these scales, although as might be expected consistency is not one of its features. Of the models proposed, that of Ref. 35 has been found to fit the measured data perhaps a little better than the others, and gives the following:

$$L_u^x = 25\, h^{0.35}/z_0{}^{0.063}\text{m}$$

$$L_u^y = 10\, h^{0.38}/z_0{}^{0.068}\text{m}$$

$$L_v^x = 5.1\, h^{0.48}/z_0{}^{0.086}\text{m}$$

$$L_w^x = L_w^y = \text{the lesser of } 0.35\, h \text{ or } 140 \text{ m} \qquad (16)$$

Representative plots shown on Fig. 13 indicate that the longitudinal and transverse scales vary quite differently with altitude.

Spectrum Shapes

As with the other characteristics of the boundary layer, measured spectrum shapes also exhibit great variability, and

‡The sign is positive here because w_g' is positive downward to be consistent with vehicle axes. A minus sign is usual in fluid mechanical and meteorological literature.

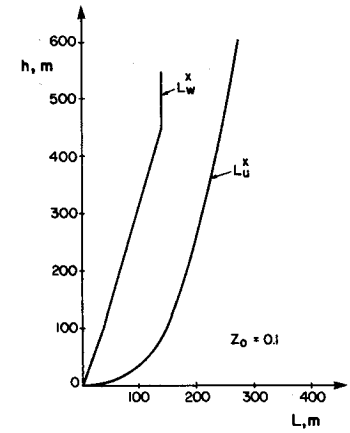

Fig. 13 Turbulence scales for ESDU model.

there seems to be no strong empirical reason to prefer one model to another. Thus it is convenient and sensible to use the von Kármán model [Eqs. (6-8)], which is as good a fit as any other, in this regime as well as at altitude. The anisotropy is commonly allowed for by using the appropriate intensity and scale in each of the one-dimensional spectra [Eqs. (7) and (8)]. Thus Eq. (7) is used for Φ_{uu} with $\sigma^2 = \sigma_u^2$ and $L = L_u^x$. Equation (8) is used for Φ_{vv} and Φ_{ww} with intensities σ_v and σ_w and scales $2L_v^x$ and $2L_w^x$, respectively. One additional spectrum is needed for $\overline{u_g' w_g'}$. This is given in Ref. 35 or UTIAS Review 44.

The Input/Response Problem

Let a linear system that approximately models the rigid and elastic degrees of freedom of the vehicle be given by

$$A_1 \dot{x}(t) = A_2 x(t) + Bu(t) + T_1 g(t) + T_2 \dot{g}(t)$$

or

$$\dot{x}(t) = Ax(t) + Cu(t) + D_1 g(t) + D_2 \dot{g}(t) \qquad (17)$$

In this form, with constant matrices, the model allows the inclusion of only quasisteady aerodynamics. This is adequate for most problems dominated by rigid-body modes (such as may occur in investigations of guidance, control, and handling qualities), but may not be adequate for problems involving significant participation of structural degrees of freedom (see Fig. 24).

The term in $\dot{g}$ is present on the right side of Eq. (17) to accommodate $\dot{w}_g$, which should be included in the gust-force terms if $M_{\dot{w}}$ is retained in the basic vehicle aerodynamics. By defining a new variable z via

$$x = z + D_2 g \qquad (18)$$

one can transform Eq. (17) into the canonical form

$$\dot{z} = Az + Cu + Dg \qquad (19)$$

This is solved in the usual way for z, and then the desired state vector x is found from Eq. (18). When Eq. (19) is used to compute time-domain solutions, no difficulty arises in using Eq. (18) to derive x from z. However, when statistics of the response are being sought, i.e., the output correlation or spectrum matrix, Eq. (18) implies

$$R_{xx}(\tau) = R_{zz}(\tau) + D_2 R_{gg}(\tau) D_2^T + D_2 R_{gz}(\tau) + R_{zx}(\tau) D_2^T \qquad (20)$$

which contains the cross correlations of the gust input and the z response. A similar relation of course exists for input-output cross-spectrum functions. Thus retaining $\dot{g}$ has the con-

sequence that either additional input correlations and/or spectra are needed, or some input-output correlations and/or spectra must be calculated. The cross correlation of g and z can readily be calculated using the convolution integral for z. The result is

$$R_{gz}(\tau) = R_{zg}(-\tau) = \int_0^\infty R_{gg}(u) \exp[A^T(u+\tau)]\,du \qquad (21)$$

When unsteady aerodynamics must be used, the problem can be formulated in either the frequency or time domains, in terms of the relevant transfer functions or impulse responses, i.e.

$$\bar{x}(s) = G(s)\bar{g}(s) \qquad (22)$$

or

$$x(t) = \int_0^t H(t-\tau)g(\tau)\,d\tau \qquad (23)$$

Here $G(s)$ is the matrix of transfer functions $G_{ij}(s)$ that relate the response variable x_i to gust variable g_j, and $H(t)$ is the matrix of impulse responses $H_{ij}(t)$ that gives the response of x_i at time t to a delta-function input in g_j at time zero. $G(s)$ and $H(t)$ are a Fourier-transform pair so that a knowledge of one, given the ready availability of FFT (fast Fourier transforms) implies a knowledge of the other. Appropriate augmented differential equations can also be used in the time domain (see below).

A comment is in order at this point about the methods used to calculate pressure distributions associated with turbulence. The approach universally employed for airplanes is to use a theory that treats the vehicle as though it were flying in still air with its surfaces in motion so as to produce a "normal-wash" boundary condition identical to that for the turbulence being simulated. It is by no means obvious that the two situations (turbulence plus no surface motion, and still air plus surface motion) produce identical air loads. Indeed, in general, they do not. However, with certain restrictions (see UTIAS Review 44) the loads *are* the same, and the restrictions are not such as to invalidate the procedure for most applications.

In the following we discuss various choices for g, and the consequences of these choices for the structure of the model.

The Uniform-Gust Approximation (Simplest Case)

The simplest case is that in which Eq. (17) is employed with the g vector made up of only the three gust components at the center of gravity (c.g.), i.e.,

$$g = [u_g v_g w_g]^T \qquad (24)$$

The implication here is that $[u_g, v_g, w_g]$ are each uniform over the airplane, and that quasisteady aerodynamics can be used. Thus the instantaneous velocity of the airplane relative to the air (the airspeed) is

$$V-(W-W_A) = [(u-u_g)(v-v_g)(w-w_g)]^T \qquad (25)$$

and the incremental aerodynamic forces and moments associated with g are, with the conventional assumptions, expressed entirely in terms of classical stability derivatives, for example, $\Delta M = -M_u u_g - M_w w_g - M_{\dot{w}} \dot{w}_g$.

The Linear-Field Approximation

In the linear-field approximation, we use the ideas discussed in relation to Fig. 5, i.e., we consider the velocities $[u_g v_g w_g]$ to be linear functions of $[x\ y\ z]$. Since most airplanes are approximately planar, we consider only such airplanes in detail. We are then interested primarily in the x and y gradients of the three component velocities in addition to their values at the mass centre. Of the six such gradients, two ($\partial u_g/\partial x$ and $\partial v_g/\partial y$) represent strains with velocity fields that would be expected to have rather small effect on the

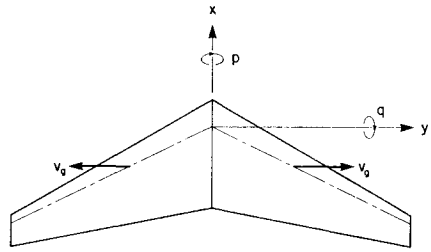

Fig. 14 Illustration of axial strain.

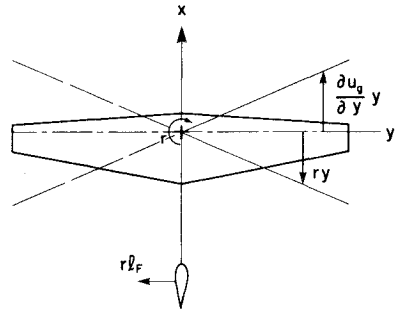

Fig. 15 The $\partial u_g/\partial y$ effect.

longitudinal aerodynamics, and none at all on the lateral aerodynamics. Consider $\partial v_g/\partial y$, for example, and its effect on a wing (Fig. 14). The perturbation velocities shown at a pair of symmetric points would act through the dihedral and sweep to produce changes only in the lift, drag, and pitching moment. These would be small and we assume they can be neglected. Thus four gradients remain: $\partial w_g/\partial x$, $\partial w_g/\partial y$, $\partial u_g/\partial y$, and $\partial v_g/\partial x$. Considering a planar airplane (Fig. 14) we see that the gust downwash at point (x, y) is

$$w_g = \frac{\partial w_g}{\partial x}x + \frac{\partial w_g}{\partial y}y \qquad (26)$$

However, if the vehicle is pitching and rolling, the contribution of its rates of rotation to the wing normal velocity at (x, y) is

$$w = py - qx \qquad (27)$$

Thus the wing boundary conditions (normal relative wind $w_g - w$) produced by Eqs. (26) and (27) are identical if $p = -\partial w_g/\partial y$ and $q = \partial w_g/\partial x$, and the wing pressure distributions will be the same whether it is rotating or exposed to the linear gust gradient. For this reason we denote

$$p_g = \partial w_g/\partial y; \qquad q_g = -(\partial w_g/\partial x) \qquad (28)$$

and treat the net effective pitch and roll rates (insofar as aerodynamic forces are concerned) as $(p-p_g)$ and $(q-q_g)$.

We now consider the remaining two gradients, and denote them by

$$r_{1g} = -(\partial u_g/\partial y); \qquad r_{2g} = \partial v_g/\partial x \qquad (29)$$

The reason for this notation is made clear by reference to Fig. 15, showing an unswept wing and fin system. The relative velocity distribution across the wing associated with $\partial u_g/\partial y$ and that associated with r are identical when $r = r_{1g}$. And the normal relative velocity at the fin associated with $\partial v_g/\partial x$ is the same as that for yaw rate r when $r = r_{2g}$. Thus the lateral aerodynamic forces for this system caused by gusts are exemplified by

$$\Delta N_g = N_{r_W} r_{1g} + N_{r_F} r_{2g} \qquad (30)$$

where subscripts W and F denote the contributions to N_r of the wing and fin, respectively. (Contributions from a propeller or jet engine intake can be handled similarly.) There are two similar expressions for ΔY_g and ΔL_g.

The swept wing is slightly more complicated. Figure 16 shows the situation. The gust gradients r_{1g} and r_{2g} yield the component relative velocities shown. The incremental force on the wing is then exemplified by

$$\Delta N_{W_g} = N_{r_{W_1}} r_{1g} + N_{r_{W_2}} r_{2g} \tag{31}$$

with similar expressions for ΔY_g and ΔL_g. The derivatives $N_{r_{W_1}}$ and $N_{r_{W_2}}$ are new and no ready source of them is available. It is of course a relatively straightforward task to generate them from the available theories for swept wings, and this is a task that needs to be carried out in order to make full use of this method. In this representation of the gust field, the input vector becomes

$$g = [u_g v_g w_g p_g q_g r_{1g} r_{2g}]^T \tag{32}$$

and there are obvious additions to the six forces and moments related to the additional inputs $p_g \ldots r_{2g}$. By way of example, for longitudinal motion, the gust vector in this model is $g = [u_g w_g q_g]$, and the gust matrices of Eq. (17) are

$$D_1 = \begin{bmatrix} (T_v - D_v) & -D_\alpha/V_e & 0 \\ L_v & L_\alpha/V_e & L_q \\ M_v & M_\alpha/V_e & M_q \\ 0 & 0 & 0 \end{bmatrix} \quad D_2 = \begin{bmatrix} 0 & 0 & 0 \\ 0 & L_{\dot\alpha}/V_e & 0 \\ 0 & M_{\dot\alpha}/V_e & 0 \\ 0 & 0 & 0 \end{bmatrix} \tag{33}$$

The linear-field approximation gives a good representation of the gust velocity distribution over the airplane only when Ω_1 and Ω_2 are "small enough," i.e., when the wave lengths λ_1 and λ_2 are considerably larger than the length and span of the airplane, respectively. We quantify this to mean $\lambda_1 \geq 10\ell_t$, $\lambda_2 \geq 10b$. The portion of the two-dimensional input spectrum that lies outside the associated bounds on Ω_1, and Ω_2 is treated only approximately. The use of this method is thus indicated when the invalid portion of the spectrum does not contribute more than say 20% of the total rms value of the response.

A flight investigation has been carried out at the National Aeronautical Establishment in Canada that provides a check on the linear-field approximation.[38] A T-33 airplane was instrumented to measure the longitudinal input variables u_g, α_g, and $\Delta\delta_e$ and the response variables V, α, θ, a_{c_x}, and a_{c_z}. It was flown at about 1000 ft altitude in turbulence of $\sigma_w \doteq 3.7$ ft/s. The measured responses to gust and pilot inputs were compared with those calculated by the linear-field approximation for a rigid airplane. The measured spectra of a_{c_z}, $\Delta\alpha$, and $\Delta\theta$ were all in quite good agreement with the calculated values, as were the rms values of the responses.

Correlations and Spectra of Gust Gradients

Reference 7 gives spectrum functions for the gust input gradients treated above, i.e., p_g, q_g, r_{1g}, and r_{2g}. These are based on the Dryden spectrum, the method of calculation being to find the spectra of the relevant slopes (such as $\partial w_g/\partial y$) at the origin. This method tends to exaggerate unduly the linear gradient effect at high wave number and indeed it was necessary to truncate the range of the wave number component Ω_2 in order to avoid infinite spectral densities. For consistency, we want the spectra of p_g, etc., that correspond to the von Kármán model, and we should like to have an approximation that is better at higher wave numbers and that

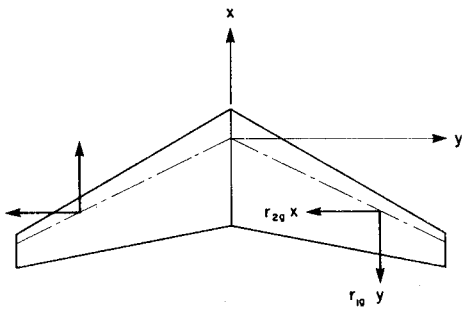

Fig. 16 Effects of r_{1g} and r_{2g} on a swept wing.

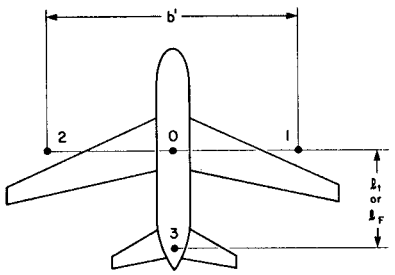

Fig. 17 The four-point model.

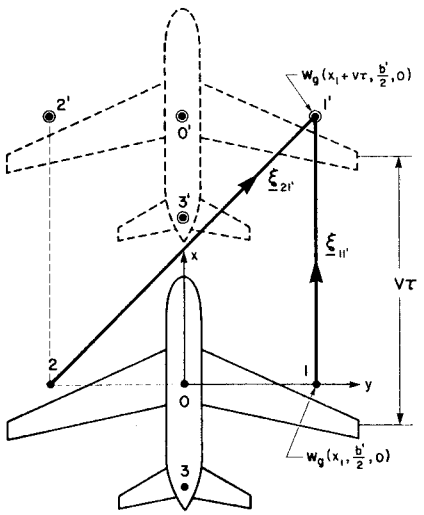

Fig. 18 Illustration of arguments of correlation function.

avoids the need to truncate a portion of the spectrum. Such an approximation is provided by the "four-point model" illustrated in Fig. 17. This is an adaptation and extension of ideas proposed by Skelton[39] and Bryson and Holley.[40] In this approach, the gust velocities at the four points shown are used to define the various gradients. For u_g and v_g we use the values at the c.g., but because w_g is so important we take it to be the average at the three wing points. By choosing points 0, 1, and 2 on a straight line, as shown, two may not be on the wing, and there is some loss in fidelity as a consequence. The inputs are then:

$$p_g = \frac{1}{b'}(w_1 - w_2) \qquad r_{1g} = \frac{1}{b'}(u_2 - u_1)$$

$$q_g = \frac{1}{\ell_t}(w_3 - w_0) \qquad r_{2g} = \frac{1}{\ell_F}(v_0 - v_3)$$

$$u_g = u_0 \qquad v_g = v_0 \qquad w_g = \frac{1}{3}(w_0 + w_1 + w_2) \tag{34}$$

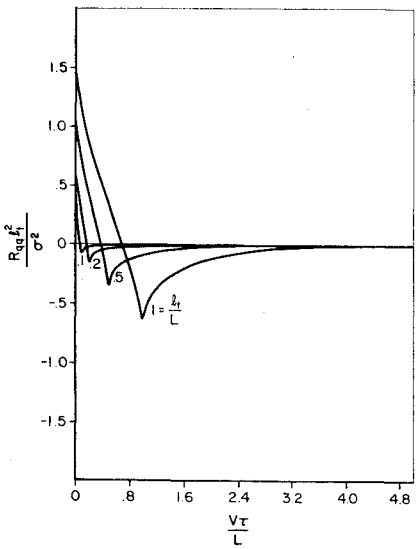

Fig. 19 Autocorrelation of the q_g input for four-point model ($\ell_t = 0.6\,b'$).

The autocorrelations and cross correlations of these seven time-varying inputs are readily calculated with the aid of Eq. (4). Consider p_g, for example. The autocorrelation is:

$$\langle p_g(t)p_g(t+\tau)\rangle = \frac{1}{(b')^2}\left[\langle w_1 w_1'\rangle + \langle w_2 w_2'\rangle - \langle w_1 w_2'\rangle - \langle w_2 w_1'\rangle\right] \tag{35}$$

where w_1 and w_2 are values of w_g at points 1 and 2 at time t, and w_1' and w_2' are values at the same wing points at the later time $(t+\tau)$ (see Fig. 18). The separation vectors between points 1 and 1′, and 2 and 1′ are illustrated in the figure by way of example. From Eq. (35), Fig. 18, and Eq. (4) we get

$$R_{pp}(\tau) = \frac{2}{(b')^2}\left[R_{33}(V\tau, 0, 0) - R_{33}(V\tau, b', 0)\right] \tag{36}$$

or

$$\frac{(b')^2}{2\sigma^2} R_{pp}(\tau) = g(\xi_1) - g(\xi_3)$$

where

$$\frac{\xi_1}{aL} = \zeta_1 = \left|\frac{V\tau}{aL}\right| \tag{37}$$

$$\frac{\xi_3}{aL} = \zeta_3 = \left[\left(\frac{V\tau}{aL}\right)^2 + \left(\frac{b'}{aL}\right)^2\right]^{1/2} \tag{38}$$

In a similar way, we get the remaining autocorrelations R_{qq}, $R_{r_1r_1}$, $R_{r_2r_2}$, and R_{ww}, and the nonzero cross correlations R_{wq}, R_{vr_1}, R_{vr_2}, and $R_{r_1r_2}$.

Graphs of two of the correlations are given as examples in Figs. 19 and 20. The associated spectrum functions (their Fourier transforms) are shown in Fig. 21. These were calculated for the von Kármán model. (The remaining correlations and spectra are given in UTIAS Review 44.) It

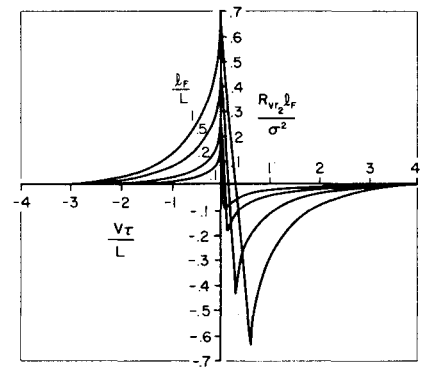

Fig. 20 Cross-correlation R_{vr_2} for four-point model ($\ell_F = 0.6\,b'$).

should be noted that all the cross correlations between the longitudinal inputs (u_g, w_g, and q_g) and the lateral inputs (v_g, p_g, r_{1g}, and r_{2g}) vanish. *Thus the traditional separation between longitudinal and lateral dynamics occurs in the linear gust response problem as well.*

The choice of b' in the four-point model is to some extent arbitrary. Probably the most important criterion to apply in choosing it is to minimize the error in the autocorrelation of the rolling moment $L_p p_g$ as compared with an exact representation.[20] Bryson and Holley[40] have found that $b' = 0.85\,b$ is a good choice from this standpoint.

Unsteady Aerodynamics

Two classical solutions exist that provide bench marks for an understanding of the unsteady aerodynamics associated with gust penetration: the Küssner function $K(t)$ [41] that gives the response to a sharp-edged gust, and the Sears function, $S(\omega)$ [11] for a sinusoidal gust—both for incompressible flow. Figures 22 and 23 show the structure of the gust and the lift response of the wing in the two cases. Since the basic underlying theory is linear, the two functions are related, i.e., $\dot{K}(t)$ and $S(\omega)$ are a Fourier-transform pair. Figure 22 shows that the two-dimensional wing travels seven chord lengths before the lift reaches 90% of its final value, and that the time lag is very much shortened for finite aspect ratio—to about three chord lengths at $A = 6$.

Figure 23 shows the lift frequency response for the sinusoidal gust. The wave number is $\Omega_1 = 2\pi/\lambda$ and the circular frequency is $\omega = 2\pi V/\lambda$. The "reduced frequency" k_1 is defined as

$$k_1 = \omega c/2V = \Omega_1 c/2 \tag{39}$$

Figure 23 indicates that an appreciable phase lag in the lift has developed at a frequency $k_1 = 0.1$, and that the lift amplitude diminishes rapidly with further increase in frequency. We may therefore reasonably take $k_1 = 0.1$ as an upper limit for the validity of quasisteady aerodynamics. The corresponding portion of the turbulence spectrum is therefore that for which

$$\Omega_1 c/2 \leq 0.1 \tag{40}$$

It is very important to note that this criterion depends on the *size* of the airplane, but *not on its speed*. The underlying reason for this is that in incompressible flow the downwash at the wing is governed by the spatial distribution of trailing vorticity and hence by the wavelength of the phenomenon, not its frequency. Expressed in terms of wavelength, Eq. (40) gives $\lambda_1/c \geq 10\pi$ or, for $\ell_t \approx 3c$, λ_1/ℓ_t must be greater than about 10. This requirement on wave length is roughly com-

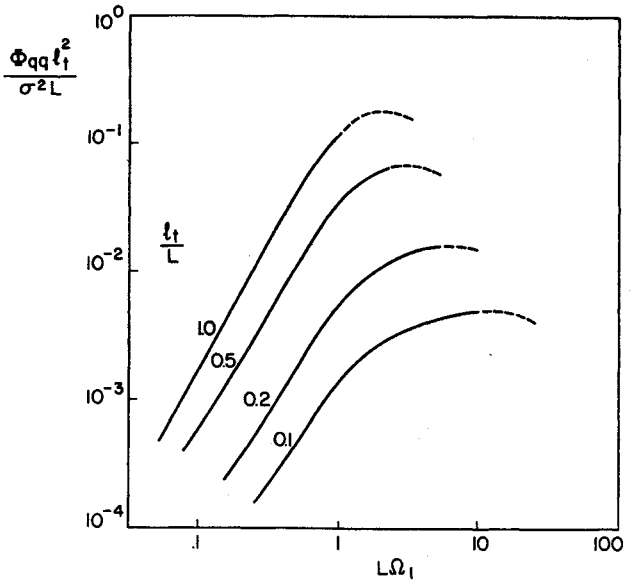

Fig. 21a Spectral density Φ_{qq} for four-point model ($\ell_t = 0.6\,b'$).

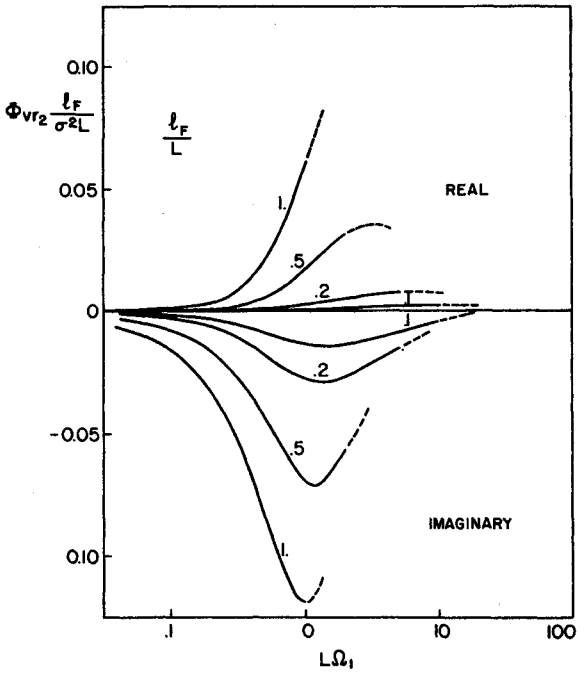

Fig. 21b Spectral density ϕ_{vr_2} for four-point model ($\ell_F = 0.6\,b'$).

patible with that for the linear-field representation described above. Thus we may as a rough general rule conclude that the quasisteady linear-field model (QSLFM) is self-consistent. The practical import of the restriction on the wave number is illustrated in Fig. 24 for an airplane of wing chord 20 ft flying in isotropic turbulence of integral scale 1000 ft. For this airplane, Eq. (40) yields $\Omega_1 \leq 0.01$ ft^{-1} as the upper limit for validity of the quasisteady aerodynamics.

Figure 24 shows the lateral and longitudinal spectrum shapes for the von Kármán model of turbulence. Representative ranges of wave number associated with different modes of response are identified on the figure, and we see that for this case (rather large airplane, moderate-scale turbulence) the range of interest extends well beyond the indicated limit. If there are significant structural mode responses, as is likely the case for wing stresses of large transports, then appreciable errors can be incurred unless unsteady aerodynamic theory is employed. This is accentuated by the presence of N_0 in Eq. (12) and the fact that it

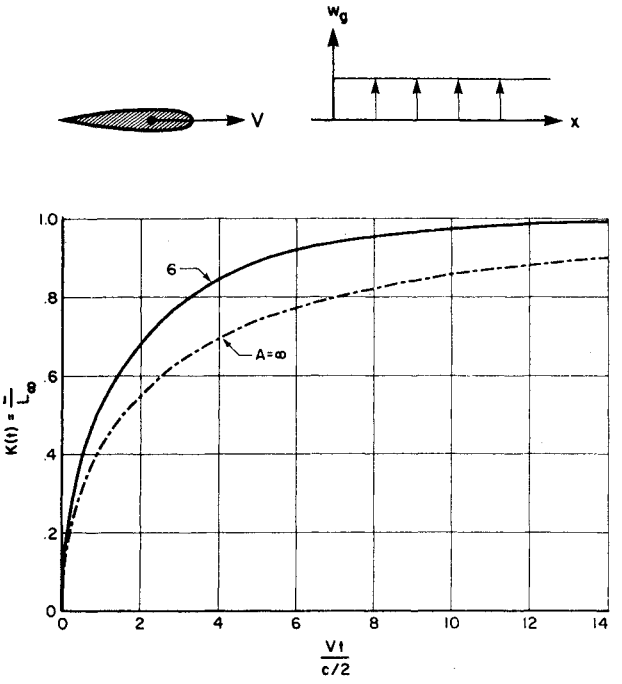

Fig. 22 The Küssner function (from NACA TN 3639).

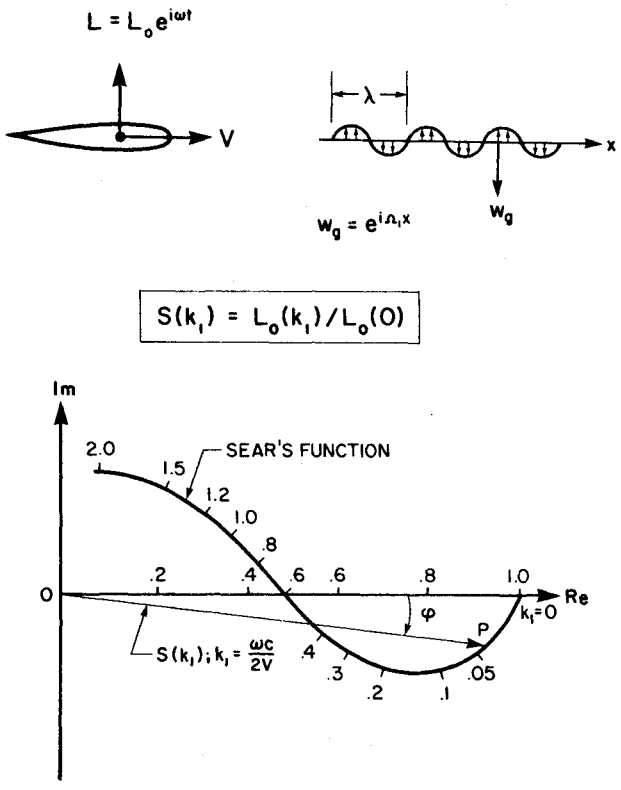

Fig. 23 Vector plot of the Sears function.

depends on the area under $\Omega_1^2\Phi(\Omega_1)$ which emphasizes the high wave number end of the spectrum.

The extension of the Sears problem to two-dimensional waves of downwash has been accomplished by Filotas.[42,43] (Figure 7 illustrates the inclined waves considered.) The lift response is of course in this case a function of Ω_2 as well as of Ω_1. Filotas has obtained approximate solutions for finite-aspect-ratio rectangular wings as well as for infinite A and gives the "generalized Sears function" as

$$S_G(k_1, k_2, A) = S(k_1)\Gamma(k_1, A)\,[2J_1(k_2)/k_2] \qquad (41)$$

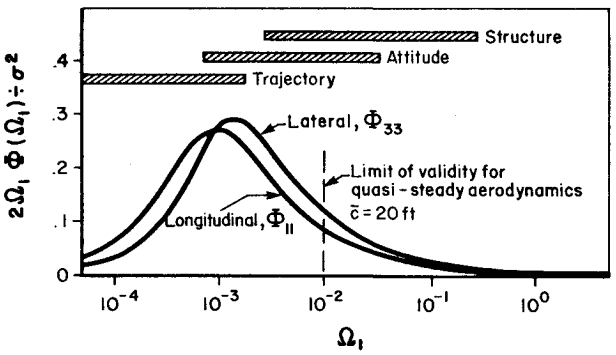

Fig. 24 One-dimensional spectra; isotropic turbulence; von Kármán model, $L = 1000$ ft.

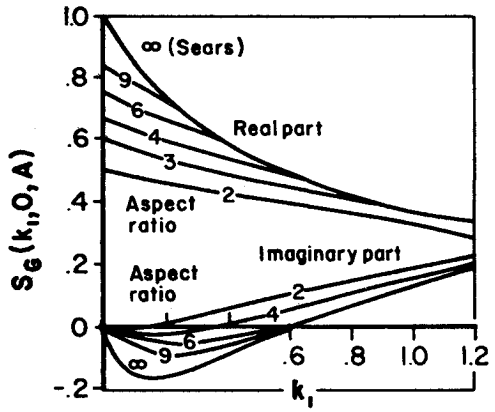

Fig. 25 Effect of aspect ratio on lift transfer function in sinusoidal downwash.

where $S(k_1) = S_G(k_1, 0, \infty)$ is the Sears' function. Both wave inclination (the k_2 effect) and finite aspect ratio reduce the lift from that associated with $S(k_1)$. Of the two, the finite-aspect-ratio effect is more important (Fig. 25) but both need to be taken into account for accurate results. T.R. Nettleton has carried out experimental measurements of $S_G(k_1, k_2, \infty)$ at the University of Toronto (unpublished). The main results are shown in Fig. 26 where the general pattern of $|S_G|^2$ predicted by theory is confirmed by the experiments, but the detailed numerical values are in only rough agreement.

Incorporating Unsteady Aerodynamics in the Mathematical Model

There are two basic approaches to including unsteady aerodynamics in a linear model, suggested by Eqs. (22) and (23). That is, computations can be in either the frequency domain or the time domain. The key to the former is a set of relevant transfer functions $G(s)$, to the latter a set of relevant differential equations and/or impulse-response functions $H(t)$. The choice of approach is governed by the intended use of the model, the proclivities of the analyst, and the particular computing capacity available. Whatever approach is used, there are choices to be made about number of degrees of freedom, sophistication of the aerodynamic submodel, and sophistication in representing the turbulence. These should all be consistent, in that the errors or uncertainties associated with each should be of the same order of magnitude. This principle is not always adhered to in that models are sometimes constructed with very large numbers of degrees of freedom, incorporating a sophisticated finite-element representation of the aerodynamics and the structure, and are then driven with relatively crude gust models.

We saw earlier that the model with quasisteady aerodynamics is roughly compatible with the linear-field approximation for the turbulence. Thus as a rough general rule one should, to be consistent, relax both these restrictions

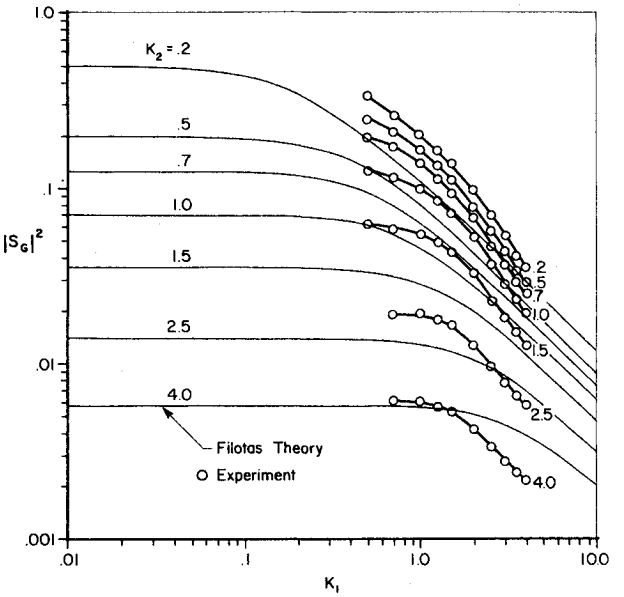

Fig. 26 Comparison of experimental $|S_G(k_1, k_2, \infty)|^2$ with theory.

at the same time. This means incorporating unsteady aerodynamics as represented by the Theodorsen or Wagner class of functions in the forces induced by vehicle motion, and by the Sears or Küssner class of functions in the forces associated with gust inputs, at the same time as a more exact spatial distribution of the gust field is included.

In the Frequency Domain

The appropriate formulation for the frequency domain, i.e., a spectral analysis, can be obtained from Eq. (17) with some changes. For the gust response problem we drop the control term (if there is a feedback controller, the $\boldsymbol{u}$ vector will be absorbed into the $\boldsymbol{x}$ vector with corresponding modifications to A_1 and A_2) and write the equation in frequency response form:

$$[i\omega A_1(\omega) - A_2(\omega)]X(\omega) = F(\omega) \tag{42}$$

Here we explicitly show that A_1 and A_2 may be functions of frequency by virtue of frequency-dependent structural damping and by virtue of replacing constant aerodynamic derivatives (such as L_α) by aerodynamic transfer functions such as $G_{L_\alpha}(\omega)$ (see Ref. 6, Sec. 5.11). $X(\omega)$ and $F(\omega)$ are, respectively, the complex amplitudes of $\boldsymbol{x}(t)$ and $\mathfrak{F}(t)$ when the latter are sinusoidal, and $\mathfrak{F}(t)$ is the vector of periodic generalized forces produced by a sinusoidal gust. From Eq. (42), one can readily find X when F is known, as

$$X(\omega) = [i\omega A_1 - A_2]^{-1} F \tag{43}$$

The central problem in this calculation is of course to find F. To this end one uses the basic spectral component of turbulence defined in Eq. (2) and illustrated in Figs. 6 and 7. We specialize at once to the case of the planar airplane and hence to a two-dimensional wave, for which the gust downwash is given by Eq. (3). Similar expressions of course apply for u_g and v_g. There are now available sophisticated panel methods for computing the periodic aerodynamic load distribution over the surfaces of an airplane experiencing periodic relative normal velocities at its surface. The doublet-lattice method developed by Rodden and others is one such.[44,45] There also exist powerful multipurpose computing programs for carrying out the necessary calculations.[46] The program of Ref. 46 allows up to 70 structural degrees of freedom, and up to 400 aerodynamic singularities. With such theories and programs, one can calculate F for any spectral component of turbulence. Now consider a wave of downwash w_g of unit

amplitude, $w_g = e^{i\Omega_1 Vt} e^{i(\Omega_1 x + \Omega_2 y)} = e^{i(\omega t + \varphi)}$, with frequency $\omega = \Omega_1 V$ and phase angle $\varphi = \Omega_1 x + \Omega_2 y$. Let the vehicle surface be subdivided into N panels, at each of which there is a normal gust velocity amplitude of $\boldsymbol{n}^T \boldsymbol{k} e^{i\varphi}$ where $\boldsymbol{n}$ is a unit vector normal to the panel and $\boldsymbol{k}$ the unit vector on the body-fixed axis oz. The phase φ of this periodic downwash depends on the location of the element. Let the set of N such complex normal velocity amplitudes be the N vector $\boldsymbol{v}$. Let the resulting normal force amplitudes at the N panels be given by the N vector $\boldsymbol{f}$. Then the computer program will yield the aerodynamic matrix A that connects force with gust:

$$\boldsymbol{F} = A\boldsymbol{v} \tag{44}$$

From the N elements of $\boldsymbol{f}$ one then constructs the M vector $\boldsymbol{F}$ of Eq. (43) via a matrix $\boldsymbol{P}$, all of whose elements are geometric (containing such items as the direction cosines of the normal to the element, the position vector of its singularity, and its normal deflection in each elastic mode). Thus finally

$$\boldsymbol{F} = \boldsymbol{P}\boldsymbol{f} = \boldsymbol{P}A\boldsymbol{v} \tag{45}$$

and $X(\omega)$ is obtained from Eq. (43). This process can of course in principle be carried out for each of u_g, v_g, and w_g gusts. The existing panel methods are based on a uniform steady incident flow, and satisfy a suitable time-dependent "normal wash" boundary condition. Thus they implicitly allow for v_g and w_g, but not u_g. The effect of u_g can be partly allowed for by modifying the boundary condition, but this is not the whole correction. The existing theories need to be extended to include a small u_g field exactly. The system responses to the sinusoidal wave are functions of Ω_2 as well as of $\omega = \Omega_1 V$. We designate the response in the ith state variable as

$$X_{iu}(\Omega_1, \Omega_2),\ X_{iv}(\Omega_1, \Omega_2),\ X_{iw}(\Omega_1, \Omega_2) \tag{46}$$

so that for example X_{iw} is the complex amplitude of the periodic $x_i(t)$ that results from a unit sinusoidal downwash having wave number (Ω_1, Ω_2). As first presented by Ribner,[17] this theory applied only to a single gust component, w_g. It was noted in Ref. 6 (p. 555) that the method had not been explicitly extended to cover simultaneous inputs of u_g, v_g, and w_g. This limitation has now been removed, and it has been shown (UTIAS Review 44) that the usual relations between input and output spectra for a one-dimensional process [e.g., Ref. 6, Eq. (3.4), p. 48] apply to this case as well. Thus, explicitly we get the two-dimensional spectra of x_i as

$$\Psi_{x_i x_i}(\Omega_1, \Omega_2) = |X_{iu}|^2 \Psi_{uu}(\Omega_1, \Omega_2) + |X_{iv}|^2 \Psi_{ww}(\Omega_1, \Omega_2) + |X_{iw}|^2 \Psi_{ww}(\Omega_1, \Omega_2) + 2Re\{X_{iu} X_{iv}^* \Psi_{uv}(\Omega_1, \Omega_2)\} \tag{47}$$

Equation (47) contains only one cross spectrum; for isotropic turbulence, the other two can be shown to vanish. The three input power spectra in it are given by Eqs. (13.2) and (13.17) of Ref. 6, and the cross spectrum is given in UTIAS Review 44. To find quantities such as $\bar{A}$ and N_0 needed for design in Eq. (12) we need the one-dimensional response spectrum

$$\Phi_{x_i x_i}(\Omega_1) = \int_{-\infty}^{\infty} \Psi_{x_i x_i}(\Omega_1, \Omega_2)\, d\Omega_2; \quad \omega = V\Omega_1 \tag{48}$$

When the u_g input is really negligible, as it is in some situations, then the cross spectrum in Eq. (47) is not needed, and only the v_g and w_g spectra remain. When spanwise variation of gust is also neglected, then the two-dimensional spectrum functions are not needed, the implicit assumption being that

$$\Phi_{x_i x_i}(\Omega_1) = |X_{iu}(\Omega_1, 0)|^2 \Phi_{uu}(\Omega_1) + |X_{iw}(\Omega_1, 0)|^2 \Phi_{ww}(\Omega_1) \tag{49}$$

It is certainly tempting to use Eq. (49) instead of Eq. (47) to calculate response spectra, since the computing time is much less. However, no general comment can be made about the loss of accuracy incurred by so doing. This assessment needs to be made in each case.

In the Time Domain

One class of time-domain solutions is accomplished by convoluting impulse response functions as in Eq. (23). For gust response this is useful only when the spanwise variation of the gust is neglected. For then the inverse Fourier transform of the frequency response function $X_{iw}(\Omega_1, 0)$ is the response $H_{iw}(Vt)$ to an impulsive gust $w_g(Vt) = \delta(Vt)$. This can be used for calculating response to $(1 - \cos)$ or other discrete-gust forms. There are however situations when convolution of impulse or step responses may not serve the need, as in real-time simulation problems. These generally require modeling in a form that can be mechanized so that vehicle and operating parameters can be changed without too much difficulty, for example mechanization by differential equations. Such is not the case with impulsive admittances that are obtained by Fourier-transforming frequency responses. Fortunately, the QSLFM is good enough for most simulator work, so differential equations are readily available that do not include unsteady aerodynamics effects.[46-48] For the details, the reader is referred to UTIAS Review 44.

The Landing Problem

The problem of analyzing the perturbations of the state vector—more particularly the trajectory—of a vehicle approaching a runway through a turbulent shear layer can be very different from those discussed above, in which we assumed explicitly or implicitly that the random process is stationary. For CTOL airplanes making relatively high-speed approaches in the absence of anomalous shear, the flight can be treated approximately by patching together several segments, each a stationary process representing passage through a homogeneous but anisotropic layer of some thickness such as 100 ft. The methods for stationary processes discussed above can be adapted in fairly obvious ways to this case. For steeper descent paths, such as those of STOL and VTOL airplanes, with lower flight speeds that accentuate the flight-path response to turbulence and shear, it is necessary to use a nonstationary analysis. This problem has been discussed in Refs. 8-10, 49, and 67 where it is pointed out that the total dispersion of the state vector from its desired value at a decision point comes from three sources: initial errors, mean wind profile (shear), and turbulence. If the human or automatic pilot provides a reasonably tight closure of the external guidance loop, the initial errors at the beginning of the descent should not contribute appreciably to the final errors. This contribution can therefore reasonably be ignored for controlled landings. The mean wind shear is a deterministic phenomenon and calls for a solution in the time domain of the time-varying equations of motion. Frost et al.[50] have recently convincingly demonstrated that automatic control of the elevator and throttle can suppress flight-path deviations in the vertical plane even in the presence of severe thunderstorm conditions.

The perturbations caused by turbulence have to be treated as a nonstationary random process. In the landing problem we are primarily interested in the trajectory of the c.g. and the aircraft speed and attitude at the decision point. For this class of problem it is probably sufficient to use the QSLFM with the time variability produced by the shear included. When the shear is small enough, a constant-coefficient linear system can be generated for the perturbations. When the shear is too large to use constant coefficients, linearity with respect to perturbations can still be retained, but one must then calculate from the basic time-varying differential equations a set of impulsive admittances $H(T, t)$ associated with the gust inputs at a number of points on the nominal descent path. The final

state vector is then given by convolution:

$$x(T) = \int_0^T H(T, t)g(t)\,dt \tag{50}$$

and the mean-square perturbations by the diagonal of

$$R_{xx}(T) = \langle x(T)x^T(T)\rangle$$

$$\equiv \int_0^T \int H(T, \alpha)\Re_{gg}(\alpha, \beta)H^T(T, \beta)d\alpha d\beta \tag{51}$$

Here $\Re_{gg}(\alpha, \beta)$ is a "constrained" cross correlation of the turbulent inputs experienced during the descent, i.e.,

$$\Re_{gg}(\alpha, \beta) = R_{gg}[r(\alpha), r(\beta), \alpha - \beta] \tag{52}$$

where $r(\alpha)$ and $r(\beta)$ are the positions reached by the airplane at times α and β after the initiation of the descent. Equation (51) contains one element, $H(T, \alpha)$, that can be calculated for a set of values of α from the basic system differential equations and another, $\Re_{gg}(\alpha, \beta)$, that must either be generated from an analytic model of the boundary layer or obtained from measurements. A facility for making these measurements is described in Ref. 9. It is expected that for boundary layers without anomalous shear, continued research in this area will lead to a reasonable analytical model for $\Re_{gg}$.[49,67]

The results of the calculation are the mean squares (ensemble averages) of the state variables [the diagonal of $R_{xx}(T)$]. These are an adequate measure of the departures from the desired state. For example, if we assume that the distribution is Gaussian, we can calculate the probability of exceeding any specified margin. One approach to the design and certification of autolanding systems would therefore be to specify a wind and Gaussian turbulence environment and maximum probabilities of exceeding certain limits on c.g. position, velocity vector, and attitude at the beginning of the flare. The non-Gaussian character of real turbulence can be compensated for in the choice of probability specified.

A very interesting and promising recent development seeks deterministic "worst-case" wind profiles for the landing case.[51,52] These profiles implicitly contain both the shear and turbulence components and are only loosely connected with observational data on the wind. They may ultimately offer the most rational basis for the design and certification of autolanding systems. Van der Vaart's[51] method finds the wind time history, subject to a constraint on the integral of its square, that maximizes a single state variable at the final time. The governing equation used is linear and time invariant and hence implies a specified control law. Markov[52] includes an unspecified controller and treats the wind and the controller as adversaries using differential game theory. This yields the design of a controller that is optimal in some sense simultaneously with the determination of the worst wind for that controller. Markov's method also has the potential to be developed for use in flight simulators.

Representation in Flight Simulators

Much effort has been devoted to the representation of turbulence in flight simulators, and the degree of physical realism needed remains a controversial issue. The simplest representation, and one commonly employed in the past, is to use filtered white noise shaped to the Dryden or von Kármán spectrum and use it in the uniform gust approximation on one or more axes. This produces a rather "bland" task for pilots, who report that it does not feel like "real" turbulence. In spite of this lack of realism, pilot ratings on the Cooper-Harper scale show the expected trends with increasing turbulence intensity. There are several potential deficiencies in this approach:

1) The pitching, rolling, and yawing associated with q_g, p_g, and r_g are absent.

2) The Gaussian distribution is unrealistic—the "intermittency" and "patchiness," the surprise element characteristic of real turbulence, is missing.

3) In simulations of landing through a boundary layer, the inhomogeneous nature of the turbulence needs to be reflected in a statistically nonstationary process for the airplane.

4) Anisotropy and boundary-layer shear both lead to the inputs being attitude dependent (see Ref. 6, Sec. 9.9). Moreover, the shear has the additional effect of influencing the basic stability of small perturbations, which should also be included in the simulation if high fidelity is sought.

5) Since the wind and turbulence are related to Earth-fixed axes, the components on vehicle axes depend on heading relative to the wind and on the angles of pitch, roll, and yaw. A realistic landing model should ideally take this into account and transform the turbulence from Earth-fixed to vehicle axes prior to calculating aerodynamic forces.

Various attempts to improve the probability distributions of the models have been made[53-57] with varying success. There seems to be little doubt that pilots will judge the non-Gaussian models to be more realistic.[58] Nevertheless, this is not necessarily translated into differences in their Cooper-Harper ratings, particularly if the different simulations are compared on the basis of the intensity of their severest patches rather than on overall intensity.[59] If the simulation has high fidelity with respect to all the other features mentioned above, and if care is taken not to clip the peaks of the signals up to say 5σ, then the non-Gaussian feature may well prove to be of secondary importance.

A method that has not received much attention, not as much in my view as it deserves, is the use of records of natural turbulence obtained in wind tunnels or in the atmosphere. These could in principle be multichannel records associated with the four-point representation of the QSLM, and hence have the correct cross correlations automatically. They could be amplitude- and time-scaled during the simulation to allow for changing speed of the airplane and changing scale and intensity of the turbulence arising from vertical stratification. Wind-tunnel simulations of the turbulence applicable to the landing problem are already in existence,[8,67] and laser Doppler anemometry may make the measurement feasible.

Passenger Comfort

The most obvious impact of turbulence on the traveling public is the rough ride it produces, accompanied by minor irritations such as coffee in the lap, more serious discomfort such as airsickness, and even occasional bodily injury. Ride roughness is not however an isolated parameter. Jacobson et al.[60] have produced a quite sophisticated model of "trip comfort" which can be expressed in the form

$$C_{\text{trip}} = \sum_{E=1}^{n} E^{1/4} C_E \Big/ \sum_{E=1}^{n} E^{1/4}$$

Here E represents the ride segment (sequentially numbered) and C_E the comfort rating associated with that segment. C is expressed on a seven-point scale from 1 = very comfortable to 7 = very uncomfortable. Approximately 80% of passengers are "satisfied" with the ride at rating 4. The contributions to C come from turbulence, maneuvers, noise, temperature, rate of climb, and seating. The turbulence comfort criterion is expressed in terms of σ_{a_z} and σ_{a_y}, the rms accelerations at the passenger location. In the absence of any other factors, the envelope shown in Fig. 27 is for "neutral" rating of ride roughness. This provides some guide to the level of response that should be provided. The designer must of course also give consideration to the deterioration in comfort that arises from

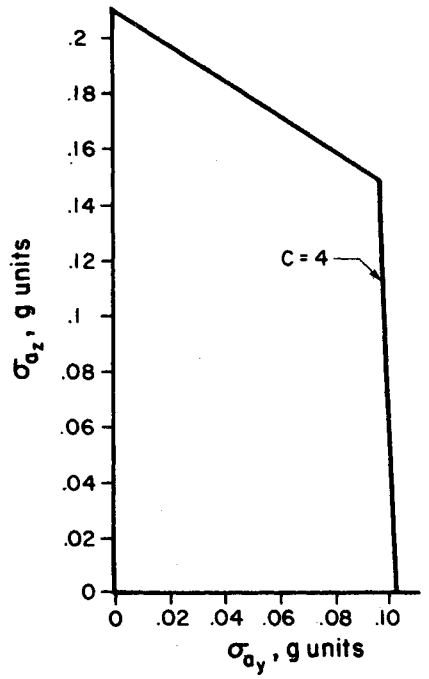

Fig. 27 Acceleration boundary for neutral passenger comfort, turbulence alone.

the joint action of the other factors mentioned above, and to the probability of occurrence of any turbulence level on the routes to be flown.

The frequency content of seat motion is also a factor in comfort. Motion sickness is generally associated with $f<1$ Hz, and other physiological responses such as elevated heart rate and sweating with higher frequencies.[61]

Gust Alleviation

Since the response of the airplane to turbulence is generally undesirable, whether from the point of view of structure, passenger, or pilot, there is substantial motivation to improve airplanes by reducing this response. It has long been known that alleviation of vertical acceleration could be achieved by feeding back longitudinal response variables to the elevator angle.[62,63] This is effective only at relatively low frequencies, because of the time lags associated with the pitching inertia of the vehicle. The needed change in wing lift can come only after the angle of attack has been changed and the subsequent aerodynamic transient has run its course. Thus this approach does not have the potential to make significant improvements in the most uncomfortable frequency range of acceleration, i.e., $f>1$ Hz. Much better results can be obtained with DLC (direct lift control), for example when ailerons, wing flaps, or spoilers are used to produce a more rapid change in lift. Insofar as rotations are concerned, the three conventional flying controls can rapidly generate moments capable of counteracting gust-induced moments. The ailerons, rudder, elevator, flaps, and spoilers can also be used to suppress structural modes, not only for gust response, but for flutter as well.[64]

The intriguing question arises as to whether turbulence effects can in principle be totally eliminated. Rynaski has studied this question[65,66] and notes the theoretical possibility, but practical impossibility of achieving this result. He examines a system such as Eq. (17) but without the $\dot{g}$ term and notes that if the sum of the control and gust terms vanishes then there is no "net forcing" term at all! If this could be realized in practice, then the controls would exactly cancel the gusts. Two conditions have to be met for this possibility to exist: 1) that a continuous accurate measurement of $g(t)$ is available and 2) that there is an open-loop control law of the form

$$u=-B^{-1}T_1 g \tag{53}$$

Now the input vector of the QSLFM [Eq. (32)] could in principle be measured by a set of sensors mounted at appropriate locations, so that condition 1 might be met to a reasonable degree of approximation, but condition 2 is possible only if the matrix B has an inverse. This implies that B is square, i.e., that there are as many controls (elements of u) as there are states (elements of x). This is manifestly not a reasonable proposition if there are any structural modes present in x. On the other hand, if there are only rigid-body degrees of freedom, if the speed degree of freedom is suppressed, and if the three controls are augmented by DLC, then the longitudinal forces [ΔZ, ΔM] induced by gust could in principle be canceled by DLC and elevator angle, but [ΔY, ΔL, ΔN] of the lateral motion could not all be canceled by rudder and aileron alone. To this end it would be necessary to add a side-force generator as well (as on CALSPAN's TIFS aircraft).

If the driving term (controls plus gusts) cannot be reduced to zero, it can however in a suitable sense be minimized, for example by minimizing the quadratic form

$$(Bu+T_1 g)^T Q(Bu+T_1 g) \tag{54}$$

in which Q is an arbitrarily chosen diagonal weighting matrix. This leads to the control law[65]

$$u=-(B^T QB)^{-1}B^T QT_1 g \tag{55}$$

The implementation of Eq. (55) would minimize the gust response according to the chosen Q.

A more precise appreciation of how the control law affects the various natural modes of response is obtained by converting the governing equation to characteristic coordinates. The result is (UTIAS Review 44)

$$\dot{q}=\Lambda q+(U^{-1}C)u+(U^{-1}D_1)g \tag{56}$$

in which Λ is the diagonal matrix of the eigenvalues λ_i. This equation uncouples the degrees of freedom, each q_i (more precisely each real one or each conjugate complex pair) describing one natural mode of the system. The important point is that $U^{-1}C$ and $U^{-1}D$ then define how each uncoupled mode is driven by each controller and by each gust input, respectively. This gives explicit guidance to the designer for sensor deployment and controller design in the light of the selection made of modes to be suppressed as expressed in Q. This approach to gust alleviation is *open loop*. It entails measuring g, knowing B and T_1 (or C and D_1) and actuating the controls according to the computed set of gains. It has to be recognized that this approach runs the risk that errors in the measurement of g, or in the foreknowledge of the elements of U, C, and D_1, can lead to a larger response than anticipated. Such errors and factors such as unknown phase lags in sensors, actuators, and aerodynamic response can actually lead to a response larger than if no control were used at all, particularly at the high-frequency end of the spectrum.

The above is to be contrasted with a pure feedback control in which some state variables are measured and used to set the controls, i.e., $u=Hx$ so that the system equation becomes

$$A_1\dot{x}=(A_2+BH)x+D_1 g$$

H would then be chosen to minimize some quadratic measure of x or of x in linear combination with u. A linear optimal control[66] can be generated that combines both open-loop and feedback elements and that is superior to either alone. Figure 28 shows an example case[66] in which the spectrum of normal acceleration at the pilot station ($\Phi_{n_{z_p}}$) is shown with and without gust alleviation. The controls used were elevator

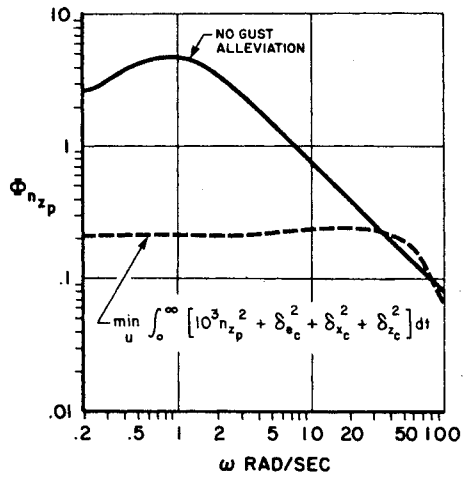

Fig. 28 Linear optimal design of gust-alleviation controller (Ref. 66).

(δe_c), flap (δz_c), and throttle (δx_c) and the quantity minimized was the integral shown. The loss in performance shown at high frequency is a result of actuator phase lags. However, the effects of aerodynamic time lags were not included in the example (the Küssner and Wagner effects) so the high-frequency portion of the response may not be reliable. Fortunately, the time lag in force buildup following a control deflection is partially compensated for by that following the onset of a gust, so the net effect of the unsteady aerodynamics is mitigated.

When gust alleviation is applied to improve ride comfort, tradeoffs will be needed to allow for the fact that rms vertical and lateral accelerations vary along the length of the fuselage owing to the presence of pitch and yaw rates and body bending. The term $x\dot{q}$ in the vertical acceleration can be just as large as the acceleration at the c.g. The use of the flying controls for this purpose is almost certain to increase the stresses in some portions of the structure, increasing the rate of accumulation of fatigue damage in some areas, while at the same time reducing it in others.

Conclusions

Our knowledge of the turbulent wind and of how to design aircraft to cope with it has grown steadily over the eight decades of powered flight since the Wrights. As a result, airplanes have become both safer and more economical, and are capable of flying under more adverse conditions. This development has been evolutionary, and with the possible exception of the influence of digital computers, has not been marked by any dramatic breakthroughs. The future is likely to follow a pattern much like that of the past.

Research in the atmosphere itself is costly and proceeds slowly. We can expect to see a continuation of flight research on the properties of turbulence at all altitudes to refine the statistics of occurrence and to probe more deeply into its structure. The latter will likely see flight measurements made with two probes separated in the spanwise direction, so as to add data on spanwise gradients of u_g, v_g, and w_g. This is important additional information, not only in relation to rolling and yawing moments, but also if the question of organized structures in the flow is to be pursued further, for simultaneous information on $\partial v_g/\partial x$ and $\partial u_g/\partial y$ will tell us something about vorticity, a feature that cannot be confirmed from only one such gradient. The elusive scale length L will continue to be hunted, probably without definitive success, for in the final analysis it depends on arbitrary choices of bandwidth and analysis method. In the boundary layer, we will no doubt see more data collected on the wind fields associated with extreme weather conditions for application to studies of landing conditions. The "worst-case" philosophy is likely to exert a strong influence on future research. For structural design this means defining ranges and associated probabilities for scale length L as well as for intensity σ; and for landing, it means finding the most adverse profiles of wind with height for a particular configuration of vehicle plus guidance plus control. The atmospheric boundary-layer wind tunnel is a facility that may be expected to contribute to knowledge of the landing environment, particularly where local features of terrain and buildings are such as to generate flows over the approach path and runway that need to be studied. This facility also has the potential to be a source of turbulence signals collected, stored, and later played back with suitable variable time and amplitude scalings as input to flight simulators or to computer models of automatic landing systems.

In the application of gust information to structural design, there will no doubt continue to be controversy on the relative merits of power-spectral-density methods and discrete gust methods, and on how well each represents the real physics of the atmosphere. This controversy will not be resolved in favor of one or the other—both techniques have their place in the spectrum of design and analytical tools and both represent aspects of reality. The degree of sophistication of the aerodynamic and structural representations used in design depends very much on whether the issue is one of structure or of guidance and control. For the former, it is generally necessary to allow for structural modes, making it essential to include many degrees of freedom and unsteady aerodynamics. For guidance and control of flight path and attitude, few degrees of freedom and the quasisteady linear-field model (QSLFM) will normally be good enough. Of course when active controls are being used to suppress structural response, the distinction between structure and control disappears and unsteady aerodynamics is needed. The cost and complexity of analysis is much higher when elaborate unsteady aerodynamics must be included, so the decision as to when, and with what fidelity, to do so is an important one. It is only fairly recently that the theoretical and computational tools to do this in practice have become widely available, and these will no doubt see further significant evolution.

There is a divergence of opinion about simulation of turbulence in piloted flight simulators. Those used by airlines for pilot training evidently do not need sophisticated high-fidelity representation of turbulence to achieve their goals. Nevertheless, new models are evolving in that direction. Simulators used for design of control systems or for research on handling qualities do need to be convincing to test pilots. Just what constitutes the necessary degree of fidelity is not yet clear. Some workers place great stress on the non-Gaussian feature of real turbulence. Others regard this as of less importance provided that other aspects of the simulation, such as visual and motion cues, multiaxes input, coordinate transformations, etc., are faithfully reproduced.

Progress can be expected in gust alleviation through active control applied to give passengers a better ride, to reduce pilot load, and to increase the fatigue life of the structure. Perfect gust alleviation is of course impossible, not only because of limitations on sensing and actuating devices, but because it is inherent in flexible vehicles that alleviation designed to reduce motion ol stress in one part of the airplane will inevitably increase it somewhere else.

As to the application of new information about turbulence and new methods of analysis to design and certification, one must be aware of the current environment in which changes take place. This environment is characterized by giant manufacturing industries and airlines, heightened public awareness and concern (the Nader syndrome), and strong government regulatory authorities. These constitute institutional constraints that contribute to inertia and rigidity. Operators resist changes that increase capital or operating costs or the complexity of operations, manufacturers resist changes that may add weight or complexity to vehicles or

increase design or manufacturing costs, and the regulatory agencies are understandably nervous about changes that have the potential, real or apparent, to affect safety adversely. In this context, one may expect the closest scrutiny of proposals to change any of the gust design methods or numerical parameters. The necessity to insure that changes in approach are carefully validated against prior art provides protection against unsafe innovations, but can also inhibit changes that could save weight without adversely affecting safety. The virtual absence of failures of primary structure in transport airplanes in recent years attributable to inadequate design loads is certainly a cause for satisfaction. It may also be evidence that there is room for further weightsaving without reducing safety. Our objective in seeking more knowledge of the atmosphere and better methods of analysis and design is of course ultimately to improve the combination of safety, economy, and comfort in air travel. The tradeoffs between these are a matter of public policy and social acceptance, not necessarily of engineering judgment. (The only absolutely safe airplane would never leave the ground!) Every improvement we can make offers the opportunity for payoff, whether collected in safety, economy, or comfort. Our profession has been generating these payoffs steadily over the years, so that we can fairly claim that a principal adversary of aviation, i.e., the turbulent wind, has been confronted, held at bay, and forced to retreat. Nevertheless, there still remain important problems to be solved and significant gains to be achieved.

References

[1] Wright, O., "How We Invented the Airplane," edited by F.C. Kelly, *Harpers Magazine,* June 1953.

[2] Wilson, E.B., "Theory of an Aeroplane Encountering Gusts," NACA Rept. 1, Pt. 2, 1915.

[3] Etkin, B., "Turning in a Wind," *Engineering Journal* (Canada), March 1945.

[4] Etkin, B., "Effect of Wind Gradient on Glide and Climb," *Journal of Aeronautical Sciences*, June 1947.

[5] Etkin, B., "A Theory of the Response of Airplanes to Random Atmospheric Turbulence," UTIAS Report 54, 1958, and *Journal of Aeronautical Sciences*, July 1959.

[6] Etkin, B., *Dynamics of Atmospheric Flight,* John Wiley & Sons, New York, 1972.

[7] Etkin, B., "Theory of the Flight of Airplanes in Isotropic Turbulence; Review and Extension," University of Toronto, UTIAS Report 72, Feb. 1961 (presented at AGARD Symposium, Brussels, April 1961, and published as AGARD Report 372).

[8] Etkin, B., Johnston, G.W., and Teunissen, H.W., "Measurement of Turbulence Inputs for V/STOL Approach Paths on a Simulated Planetary Boundary Layer," University of Toronto, UTIAS Report 189, July 1973.

[9] Etkin, B. and Teunissen, H.W., "A Method for the Estimation of Flight Path Perturbations During Steep Descents of V/STOL Aircraft," *CASI Transactions*, Vol. 2, Sept. 7, 1974, pp. 60-68.

[10] Etkin, B., Reid, L.D., Teunissen, H.W., and Hughes, P.C., "A Laboratory Investigation into Flight Path Perturbations During Steep Descents of V/STOL Aircraft," USAF Tech. Rept. AFFDL-TR-76-84, Aug. 1976.

[11] Sears, W.R., "Some Aspects of Non-stationary Airfoil Theory and Its Practical Application," *Journal of Aeronautical Sciences*, Vol. 8, 1941, pp. 104-108.

[12] Press, H. Meadows, M.T., and Hadlock, I., "Estimates of Probability Distribution of Root-Mean-Square Gust Velocity of Atmospheric Turbulence from Operational Gust-Load Data by Random-Process Theory," NACA TN 3362, 1955.

[13] Press, H. and Meadows, M.T., "A Re-evaluation of Gust-Load Statistics for Applications in Spectral Calculations," NACA TN 3540, 1955.

[14] Press, H. and Houbolt, J.C., "Some Applications of Generalized Harmonic Analysis to Gust Loads of Airplanes," *Journal of Aeronautical Sciences*, Vol. 22, No. 1, 1955.

[15] Liepmann, H.W., "Extension of the Statistical Approach to Buffeting and Gust Response to Wings of Finite Span," *Journal of Aeronautical Sciences*, Vol. 22, No. 3, 1955.

[16] Liepmann, H.W., "On the Application of Statistical Concepts to the Buffeting Problem," *Journal of Aeronautical Sciences*, Vol. 19, No. 12, 1952.

[17] Ribner, H.S., "Spectral Theory of Buffeting and Gust Response; Unification and Extension," *Journal of Aeronautical Sciences*, Vol. 23, No. 12, 1956.

[18] Diederich, F.W. and Drischler, J.A., "Unsteady-Lift Function for Penetration of Travelling Gusts and Oblique Blast Waves," IAS Preprint 714, Jan. 1957.

[19] Diederich, F.W. and Drischler, J.A., "Effect of Spanwise Variations in Gust Intensity on the Lift due to Atmospheric Turbulence," NACA TN 3920, 1957.

[20] Eggleton, J.M. and Diederich, F.W., "Theoretical Calculations of the Power Spectra of the Rolling and Yawing Moments on a Wing in Random Turbulence," NACA Rept. 1321, 1957.

[21] Houbolt, J.C., Steiner, R., and Pratt, K.G., "Dynamic Response of Airplanes to Atmospheric Turbulence Including Flight Data on Input and Response," NASA TR-R-199, 1964.

[22] Brunstein, A.I., "Clear Air Turbulence Accidents," *SAFE Journal*, Vol. 8, Jan. 1978.

[23] Disney, T.E., "C-5A Active Load Alleviation System," *Journal of Spacecraft and Rockets*, Vol. 14, Feb. 1977, pp. 81-86.

[24] Houbolt, J.C., "Atmospheric Turbulence," *AIAA Journal*, Vol. 11, April 1973, pp. 421-437.

[25] Jones, J.G., "A Theory for Extreme Gust Loads on an Aircraft Based on the Representation of the Atmosphere as a Self-Similar, Intermittent Random Process," RAE Technical Rept. 68030, 1968.

[26] Jones, J.G., "Statistical Discrete Gust Theory for Aircraft Loads," RAE Technical Rept. 73167, 1973.

[27] Tomlinson, B.N., "Developments in the Simulation of Atmospheric Turbulence," RAE Technical Memo FS 46, Sept. 1975.

[28] Jones, J.G., "Modelling of Gusts and Wind Shear for Aircraft Assessment and Certification," RAE paper prepared for CAARC Symposium on Operational Problems, India, Oct. 1976.

[29] Roshko, A., "Structure of Turbulent Shear Flows: A New Look," *AIAA Journal*, Vol. 14, Oct. 1976, pp. 1349-1357.

[30] Lamb, Sir Horace, *Hydrodynamics*, pp. 31-32.

[31] "Military Specification-Flying Qualities of Piloted Airplanes," MIL-F-8785B, Aug. 1969.

[32] Batchelor, G.K., *Theory of Homogeneous Turbulence*, Cambridge University Press, Cambridge, England, 1953.

[33] Simiu, E. and Scanlan, R.H., *Wind Effects on Structures*, John Wiley & Sons, N.Y., 1978.

[34] Teunissen, H.W., "Characteristics of the Mean Wind and Turbulence in the Planetary Boundary Layer," University of Toronto, UTIAS Review 32, 1970.

[35] Engineering Sciences Data Unit, "Characteristics of Atmospheric Turbulence Near the Ground," Part II, ESDU Item 74031, 1974 and Part III, ESDU Item 75001, 1975, London.

[36] Schaeffer, D.R., "Wind Models for Flight Simulator Certification of Landing and Approach Guidance and Control Systems," *Proceedings of First Annual Workshop on Meteorological Inputs to Aviation Systems*, NASA, March 1977.

[37] Counihan, J., "Adiabatic Atmospheric Boundary Layers: A Review and Analysis of Data from the Period 1880-1972," *Atmospheric Environment*, Vol. 9, 1975, pp. 871-905.

[38] Gould, D.G., "Analysis of the Response of a Single-Engine Jet Training Aircraft During Flight in Naturally Occurring Turbulence Including the Influence of Pilot Elevator Control Input," NAE, Ottawa, Canada, private communication, 1979.

[39] Skelton, G.B., "Investigation of the Effects of Gusts on V/STOL Craft in Transition and Hover," USAF Rept. AFFDL-TR-68-85, 1968.

[40] Holley, W.E. and Bryson, A.E. Jr., "Wind Modelling and Lateral Control for Automatic Landing," *Journal of Spacecraft and Rockets*, Vol. 14, Feb. 1977, pp. 65-72.

[41] Fung, Y.C., *The Theory of Aeroelasticity*, John Wiley & Sons, N.Y., 1955.

[42] Filotas, L.T., "Theory of Airfoil Response in a Gusty Atmosphere: Part I. Aerodynamic Transfer Function," University of Toronto, UTIAS Rept. 139, 1969.

[43] Filotas, L.T., "Approximate Transfer Functions for Large Aspect Ratio Wings in Turbulent Flow," *Journal of Aircraft*, Vol. 8, June 1971, pp. 395-400.

[44] Albano, E. and Rodden, W.P., "A Doublet-Lattice Method for Calculating Lift Distributions on Oscillating Surfaces in Subsonic Flows," *AIAA Journal*, Vol. 7, Feb. 1969, pp. 279-285.

[45] Giesing, J.P., Kalman, T.P., and Rodden, W.P., "Subsonic Unsteady Aerodynamics for General Configurations: Part I, Direct Application of the Nonplanar Doublet Lattice Method," USAF AFFDL-TR-71-5, 1971.

[46] Perry, B., Krol, R.I., Miller, R.D., and Goetz, R.C., "Capabilities and Applications of a Computer Program System for

Dynamic Load Analyses of Flexible Airplanes with Active Controls (DYLOFLEX)," AIAA Paper 79-0743, 1979.

[47] Roger, K.L., "Airplane Math Modelling Methods for Active Control Design," *AGARD Conference Proceedings 228*, 1977.

[48] Ly, U.-L., "Calculation of Response Correlation Matrices for Aircraft Subjected to Three-Dimensional Turbulence," Boeing Airplane Co., private communication, Aug. 1979.

[49] Reid, L.D., Markov, A.B., and Graf, W.O., "The Application of Techniques for Predicting STOL Aircraft Response to Wind Shear and Turbulence During the Landing Approach," University of Toronto, UTIAS Rept. 215, 1977.

[50] Frost, W., Crosby, B., and Camp, D.W., "Flight Through Thunderstorm Outflows," *Journal of Aircraft*, Vol. 16, Nov. 1979, pp. 749-755.

[51] Van der Vaart, J.C., "Worst Case Time Histories Causing Largest Deviations from a Desired Flight Path," Delft University of Technology, Rept. LR-267, April 1978.

[52] Markov, A.B., "Conflict-of-Interest Wind Modelling in Aircraft Response Study," University of Toronto, UTIAS, private communication, 1979.

[53] Reeves, P.M., Joppa, P.G., and Granzer, V.M., "A Non-Gaussian Model of Continuous Atmospheric Turbulence Proposed for Use in Aircraft Design," NASA Contractor Rept. CR-2639, 1976.

[54] Jacobson, I.D. and Joshi, D.S., "Investigation of the Influence of Simulated Turbulence on Handling Qualities," *Journal of Aircraft*, Vol. 14, March 1977, pp. 272-275.

[55] Jacobson, I.D. and Joshi, D.S., "Handling Qualities of Aircraft in the Presence of Simulated Turbulence," *Journal of Aircraft*, Vol. 15, April 1978, pp. 254-256.

[56] van de Moesdijk, G.A.J., "The Description of Patchy Atmospheric Turbulence, Based on a Non-Gaussian Simulation Technique," Delft University of Technology, Dept. of Aeronautical Engineering, Rept. VTH-192, Feb. 1975.

[57] Tomlinson, B.N., "Developments in the Simulation of Atmospheric Turbulence," AGARD CP-198, 1975.

[58] Jewell, W.F., Clement, W.F., West, T.C., and Sinclair, S.R.M., "Powered-Lift Aircraft Handling Qualities in the Presence of Naturally-Occurring and Computer-Generated Atmospheric Disturbances," FAA Rept. RD-79-59, 1979.

[59] Kurkowski, R.L., NASA Ames Research Center, private communication, 1979.

[60] Jacobson, I.D., Kuhlthau, A.R., Richards, L.G., and Conner, D.W., "Passenger Ride Quality in Transport Aircraft," *Journal of Aircraft*, Vol. 15, Nov. 1978, pp. 724-730.

[61] Randel, H.W., ed., *Aerospace Medicine*, 2nd Ed., Williams and Wilkins, Baltimore, Md., 1971.

[62] McClean, R., "The Optimization of an Autopilot for an Airplane Subjected to Random Atmospheric Turbulence," University of Toronto, UTIAS Technical Note 45, 1960.

[63] Phillips, W.H. and Kraft, C.C., "Theoretical Study of Some Methods for Increasing the Smoothness of Flight Through Rough Air," NACA TN 2416, 1951.

[64] Burris, P.M. and Bender, M.A., "Aircraft Load Alleviation and Mode Stabilization (LAMS)," USAF AFFDL-TR-68-163, 1969.

[65] Rynaski, E.G., Andrisani, D., and Eulrich, B.J., "Gust Alleviation Using Direct Turbulence Measurements," AIAA Paper 79-1674, Aug. 1979.

[66] Rynaski, E.G., "Gust Alleviation-Criteria and Control Laws," AIAA Paper 79-1676, 1979.

[67] Reid, L. D., "Correlation Model for Turbulence Along the Glide Path," *Journal of Aircraft*, Vol. 15, Jan. 1978, pp. 13-20.